Role of the nonperturbative input in QCD resummed Drell-Yan Q_T distributions

Jianwei Qiu and Xiaofei Zhang
Department of Physics and Astronomy, Iowa State University, Ames, Iowa 50011
(Received 27 December 2000; published 30 April 2001)

We analyze the role of the nonperturbative input in the Collins-Soper-Sterman (CSS) *b*-space QCD resummation formalism for Drell-Yan transverse momentum (Q_T) distributions, and investigate the predictive power of the CSS formalism. We find that the predictive power of the CSS formalism has a strong dependence on the collision energy $\sqrt{S}$ in addition to its well-known Q^2 dependence, and the $\sqrt{S}$ dependence improves the predictive power at collider energies. We show that a reliable extrapolation from perturbatively resummed *b*-space distributions to the nonperturbative large *b* region is necessary to ensure the correct Q_T distributions. By adding power corrections to the renormalization group equations in the CSS formalism, we derive a new extrapolation formalism. We demonstrate that at collider energies the CSS resummation formalism plus our extrapolation has an excellent predictive power for *W* and *Z* production at all transverse momenta $Q_T \leqslant Q$. We also show that the *b*-space resummed Q_T distributions provide a good description of Drell-Yan data at fixed target energies.

DOI: 10.1103/PhysRevD.63.114011 PACS number(s): 12.38.Cy, 12.38.Qk, 14.70.−e

I. INTRODUCTION

The perturbation theory of quantum chromodynamics (QCD) has been very successful in interpreting and predicting high energy scattering processes. With new data from Fermilab run II and the CERN Large Hadron Collider (LHC) in the near future, we expect to test QCD to a new level of accuracy, and also expect that a better understanding of QCD will underpin precision tests of the electroweak interactions and particle searches beyond the standard model [1]. As pointed out in Ref. [1], the description of vector and scalar boson production properties, in particular their transverse momentum (Q_T) distribution, is likely to be one of the most intensively investigated topics at both Fermilab and the LHC, especially in the context of Higgs boson searches. It is the purpose of this paper to investigate the predictive power of QCD perturbation theory for the transverse momentum distributions of vector and scalar boson production in hadronic collisions.

The production of vector bosons ($V=\gamma^*, W^{\pm}$, and Z) with invariant mass Q at large and small Q_T in hadronic collisions has been extensively studied [1]. When $Q_T \sim Q$, effectively, there is only one hard momentum scale in the production. Therefore, we expect the fixed-order perturbative calculations in power series of α_s to be reliable [2]. In this paper, we will concentrate on the production of vector bosons at small transverse momenta, $Q_T \leqslant Q$, where the bulk of the data are. The small Q_T region also corresponds to a phase space that is most relevant to the hadronic Higgs boson production.

When $Q_T \ll Q$, the Q_T distributions calculated order by order in α_s in the conventional fixed-order perturbation theory receive a large logarithm, $\ln(Q^2/Q_T^2)$, at every power of α_s. Even at the leading order in α_s, the cross section $d\sigma/dQ^2dQ_T^2$ contains a term proportional to $(\alpha_s/Q_T^2)\ln(Q^2/Q_T^2)$ coming from the partonic subprocess: $q+\bar{q}\rightarrow V(\gamma^*, W/Z)+g$. Beyond the leading order, we can actually get two powers of the logarithm for every power of α_s, due to soft and collinear gluons emitted by the incoming partons. Therefore, at sufficiently small Q_T, the convergence of the conventional perturbative expansion in powers of α_s is impaired, and the logarithms must be resummed.

Resummation of the large logarithms in QCD can be carried out either in Q_T space directly or in the impact parameter, *b* space, which is a Fourier conjugate of the Q_T space. It was first shown by Dokshitzer, Diakonov and Troyan (DDT) that in the double leading logarithm approximation (DDLA), which corresponds to the phase space where the radiated gluons are both soft and collinear with strong ordering in their transverse momenta, the dominant contributions in the small Q_T region can be resummed into a Sudakov form factor [3]. However, the strong ordering in transverse momenta in the DDLA overly constrains the phase space of the emitted soft gluons and ignores the overall momentum conservation. As a result, the DDT resummation formalism unphysically suppresses the Q_T distributions at small Q_T [1]. By imposing transverse momentum conservation without assuming a strong ordering in the transverse momenta of radiated gluons, Parisi and Petronzio introduced the *b*-space resummation method which allows a resummation of some subleading logarithms [4]. By using the renormalization group equation technique, Collins and Soper improved the *b*-space resummation to resume all logarithms as singular as $\ln^m(Q^2/Q_T^2)/Q_T^2$ as $Q_T \rightarrow 0$ [5]. In the framework of this renormalization group improved *b*-space resummation, Collins, Soper, and Sterman (CSS) derived a formalism for the transverse momentum distributions of vector boson production in hadronic collisions [6]. This formalism, which is often called the CSS formalism, can be also applied to the hadronic production of Higgs bosons [7].

For Drell-Yan vector boson production in hadronic collisions between hadrons *A* and *B*, $A(P_A)+B(P_B)\rightarrow V(Q)+X$ with $V=\gamma^*, W^{\pm}$, and *Z*, the CSS resummation formalism has the following generic form [6]:

$$\frac{d\sigma(h_A+h_B\to V+X)}{dQ^2dydQ_T^2}=\frac{1}{(2\pi)^2}\int d^2b e^{i\vec{Q}_T\cdot\vec{b}}\tilde{W}(b,Q,x_A,x_B) + Y(Q_T,Q,x_A,x_B), \quad (1)$$

where $x_A=e^y Q/\sqrt{S}$ and $x_B=e^{-y}Q/\sqrt{S}$ with the rapidity y and collision energy $\sqrt{S}$. In Eq. (1), the $\tilde{W}$ term dominates the Q_T distributions when $Q_T\ll Q$, and the Y term gives corrections that are negligible for small Q_T, but becomes important when $Q_T\sim Q$. In the CSS formalism, the $\tilde{W}$ has the following form [6]:

$$\tilde{W}(b,Q,x_A,x_B)=\sum_{ij}\tilde{W}_{ij}(b,Q,x_A,x_B)\sigma_{ij\to V}(Q), \quad (2)$$

where $\sigma_{ij\to V}(Q)$ is the lowest order cross section for a pair of quark and antiquark of invariant mass Q to annihilate into a vector boson V, and the Σ_{ij} run over all possible quark and antiquark flavors that can annihilate into a vector boson at the Born level. In Eq. (2), the $\tilde{W}_{ij}(b,Q,x_A,x_B)$ is an effective flux to have partons of flavor i and j from the respective hadrons A and B, and it has the following form [6]:

$$\tilde{W}_{ij}(b,Q,x_A,x_B)=\mathrm{e}^{-S(b,Q)}\tilde{W}_{ij}(b,c/b,x_A,x_B), \quad (3)$$

where $S(b,Q)$ will be specified later and c is a constant of order 1 [6,8]. The $\tilde{W}_{ij}(b,c/b,x_A,x_B)$ in Eq. (3) depends on only one momentum scale, $1/b$, and is perturbatively calculable as long as $1/b$ is large enough. All large logarithms from $\ln(1/b^2)$ to $\ln(Q^2)$ in $\tilde{W}_{ij}(b,Q,x_A,x_B)$ are completely resummed into the exponential factor $\exp[-S(b,Q)]$.

Since the perturbatively resummed $\tilde{W}_{ij}(b,Q,x_A,x_B)$ in Eq. (3) is only reliable for the small b region, an extrapolation to the large b region is necessary in order to complete the Fourier transform in Eq. (1). In the CSS formalism, a variable b_* and a nonperturbative function $F^{NP}(b,Q,x_A,x_B)$ were introduced [6]:

$$\tilde{W}^{\mathrm{CSS}}(b,Q,x_A,x_B)\equiv\tilde{W}(b_*,Q,x_A,x_B)F^{NP}(b,Q,x_A,x_B), \quad (4)$$

where $b_*=b/\sqrt{1+(b/b_{max})^2}<b_{max}=0.5\ \mathrm{GeV}^{-1}$, and F^{NP} has a Gaussian-like dependence on b, $F^{NP}\sim\exp(-\kappa b^2)$ and the parameter κ has some dependence on Q^2, x_A, and x_B.

The predictive power of the CSS b-space resummation formalism relies on the following critera: (1) the Fourier transform (or b integration) in Eq. (1) is dominated by the perturbative (or small b) region, and (2) the nonperturbative input F^{NP} has a derived Q dependence when Q is large. By using data at some values of Q to fix the nonperturbative b dependence of F^{NP}, the CSS formalism predicts the Q_T distributions at different values of Q. Existing data are not inconsistent with such a form [9–13]. However, improvements are definitely needed for precision tests of the theory [1,14].

Although the b-space resummation formalism has been successful in interpreting existing data, it was argued [1,14] that the formalism has many drawbacks associated with working in impact parameter space. As listed in Ref. [1], the first is the difficulty of matching the resummed and fixed-order predictions, and the second is knowing the quantitative difference between the prediction and the fitting because of the introduction of a nonperturbative F^{NP}. In viewing of these difficulties, major efforts have been devoted to resume the large logarithms directly in Q_T space [1,14].

In this paper, we argue and demonstrate that both of these drawbacks can be overcome [8]. Since there is no preferred transverse direction, the two-dimensional Fourier transform in Eq. (1) can be reduced into a one-dimensional integration over $b=|\vec{b}|$ weighted by the Bessel function $J_0(Q_T b)$ [4,6]. We find that by using an integral form for the Bessel function, the b-space resummation formalism works smoothly for all $Q_T\leqslant Q$. Because of the smooth resummed Q_T distributions, the transition (or switch over) to fixed order perturbative calculations at large Q_T becomes less ambiguous [14].

In addition, we find that the predictive power of the b-space resummation formalism strongly depends on the collision energy $\sqrt{S}$ in addition to its well-known Q^2 dependence. Because of the steep evolution of parton distributions at small x, the $\sqrt{S}$ dependence of the $\tilde{W}$ in Eq. (1) significantly improves the predictive power of the b-space resummation formalism at collider energies. We demonstrate that the b-space resummation formalism has excellent predictive power for Drell-Yan Q_T distributions as long as Q^2 is large and/or x_A and x_B are small.

To quantitatively separate the QCD prediction from the parameter fitting, we derive a new functional form in Eq. (36) to extrapolate the perturbatively calculated b-space distribution $\tilde{W}(b,Q,x_A,x_B)$ to the large b region. Our extrapolation is derived by adding power corrections to the evolution and renormalization group equations in the CSS resummation formalism. Our extrapolation preserves the predictive power of perturbative calculations at small b, while it provides clear physical interpretations for all b dependence in the large b region. We find that the CSS b-space resummation formalism plus our extrapolation gives an excellent description of the data on the Drell-Yan Q_T distributions at both collider and fixed target energies.

The rest of this paper is organized as follows. In Sec. II, we briefly review the CSS b-space resummation formalism for the Drell-Yan transverse momentum distributions. We show that the predictive power of the b-space resummation formalism has a significant $\sqrt{S}$ dependence. In Sec. III, we quantitatively analyze the role of the nonperturbative input at large b in the b-space resummation formalism. By adding power corrections to the evolution equation of $\tilde{W}_{ij}$ and power corrections to the renormalization group equations of corresponding evolution kernels, we derive a new functional form to extrapolate the perturbatively calculated $\tilde{W}_{ij}$ to the large b region. This new functional form clearly separates the perturbative predictions in the small b region from the nonperturbative physics at large b. Finally, in Sec. IV, we numerically compare the b-space resummed Q_T distributions with experimental data. Our conclusions are also given in Sec. IV.

II. COLLINS-SOPER-STERMAN FORMALISM

In this section, we briefly review the CSS b-space resummation formalism for the Drell-Yan transverse momentum distributions. We show that the predictive power of the b-space resummation formalism has a strong dependence on the collision energy $\sqrt{S}$ in addition to its well-known Q^2 dependence. We demonstrate that the $\sqrt{S}$ dependence significantly improves the predictive power of the b-space resummation formalism at collider energies.

It was shown [6] that for $b \ll 1/\Lambda_{\rm QCD}$, the $\tilde{W}(b,Q,x_A,x_B)$ is directly related to the singular parts of the Drell-Yan Q_T distribution as $Q_T \to 0$. More precisely, the $\tilde{W}(b,Q,x_A,x_B)$ includes all singular terms like $\delta^2(\vec{Q}_T)$ and $[\ln^m(Q^2/Q_T^2)/Q_T^2]_{\rm reg}$ with $m \geq 0$. The terms that are less singular as $Q_T \to 0$ are included in the Y term in Eq. (1). The QCD resummation of the large logarithms in the CSS formalism is achieved by solving the evolution equation for the $\tilde{W}_{ij}$ [6],

$$\frac{\partial}{\partial \ln Q^2}\tilde{W}_{ij}(b,Q,x_A,x_B) = [K(b\mu,\alpha_s(\mu)) + G(Q/\mu,\alpha_s(\mu))]\tilde{W}_{ij}(b,Q,x_A,x_B), \tag{5}$$

and corresponding renormalization group equations for the kernels K and G:

$$\frac{\partial}{\partial \ln \mu^2}K(b\mu,\alpha_s(\mu)) = -\frac{1}{2}\gamma_K(\alpha_s(\mu)), \tag{6}$$

$$\frac{\partial}{\partial \ln \mu^2}G(Q/\mu,\alpha_s(\mu)) = \frac{1}{2}\gamma_K(\alpha_s(\mu)). \tag{7}$$

The anomalous dimensions $\gamma_K(\alpha_s(\mu)) = \Sigma_{n=1}\gamma_K^{(n)}(\alpha_s(\mu)/\pi)^n$ in Eqs. (6) and (7) are perturbatively calculable [6]. The renormalization group equations for K and G in Eqs. (6) and (7) ensure the correct renormalization scale dependence, $d/d\ln\mu^2[\tilde{W}(b,Q,x_A,x_B)] = 0$. The solution given in Eq. (3) corresponds to solving the evolution equation in Eq. (5) from $\ln(c^2/b^2)$ to $\ln(Q^2)$, and solving the renormalization group equations in Eqs. (6) and (7) from $\ln(c^2/b^2)$ to $\ln(\mu^2)$ and from $\ln(Q^2)$ to $\ln(\mu^2)$, respectively.

Integrating Eq. (6) over $\ln(\mu^2)$ from $\ln(c^2/b^2)$ to $\ln(\mu^2)$, and Eq. (7) from $\ln(Q^2)$ to $\ln(\mu^2)$, one derives

$$K(b\mu,\alpha_s(\mu)) + G(Q/\mu,\alpha_s(\mu)) = -\int_{c^2/b^2}^{Q^2}\frac{d\bar{\mu}^2}{\bar{\mu}^2}A(\alpha_s(\bar{\mu})) - B(\alpha_s(Q)), \tag{8}$$

where A is a function of $\gamma_K(\alpha_s(\bar{\mu}))$ and $K(c,\alpha_s(\bar{\mu}))$ while B depends on both $K(c,\alpha_s(Q))$ and $G(1,\alpha_s(Q))$. The functions A and B do not have large logarithms and have perturbative expansions $A = \Sigma_{n=1}A^{(n)}(\alpha_s/\pi)^n$ and $B = \Sigma_{n=1}B^{(n)}(\alpha_s/\pi)^n$, respectively. The first two coefficients in the perturbative expansions are known [6,9]:

$$A^{(1)} = C_F,$$

$$A^{(2)} = \frac{C_F}{2}\left[N\left(\frac{67}{18} - \frac{\pi^2}{6}\right) - \frac{10}{9}T_R n_f\right],$$

$$B^{(1)} = -\frac{3}{2}C_F,$$

$$B^{(2)} = \left(\frac{C_F}{2}\right)^2\left[\pi^2 - \frac{3}{4} - 12\zeta(3)\right] + \frac{C_F}{2}N\left[\frac{11}{18}\pi^2 - \frac{193}{24} + 3\zeta(3)\right] + \frac{C_F}{2}T_R n_f\left[\frac{17}{6} - \frac{2}{9}\pi^2\right], \tag{9}$$

where $N=3$ for SU(3) color, $C_F = (N^2-1)/2N = 4/3$, $T_R = 1/2$, and n_F is the number of active quark flavors. The functions A and B given in Eq. (9) are derived from the general expressions in Ref. [6] with the following choices for the renormalization constants: $C_1 = c = 2e^{-\gamma_E}$ and $C_2 = 1$, where $\gamma_E \approx 0.577$ is Euler's constant.

Substituting Eq. (8) into Eq. (5), and integrating over $\ln(Q^2)$ from $\ln(c^2/b^2)$ to $\ln(Q^2)$, one obtains $\tilde{W}_{ij}$ given in Eq. (3) with

$$S(b,Q) = \int_{c^2/b^2}^{Q^2}\frac{d\bar{\mu}^2}{\bar{\mu}^2}\left[\ln\left(\frac{Q^2}{\bar{\mu}^2}\right)A(\alpha_s(\bar{\mu})) + B(\alpha_s(\bar{\mu}))\right]. \tag{10}$$

In Eq. (3), all large logarithms from $\ln(c^2/b^2)$ to $\ln(Q^2)$ in $\tilde{W}_{ij}(b,Q,x_A,x_B)$ are completely resummed into the exponential factor $\exp[-S(b,Q)]$, leaving the $\tilde{W}_{ij}(b,c/b,x_A,x_B)$ with only one momentum scale $1/b$. The $\tilde{W}_{ij}(b,c/b,x_A,x_B)$ in Eq. (3) is then perturbatively calculable when the momentum scale $1/b$ is large enough, and is given by [6,12]

$$\tilde{W}_{ij}\left(b,\frac{c}{b},x_A,x_B\right) = f_{i/A}\left(x_A,\mu=\frac{c}{b}\right)f_{j/B}\left(x_B,\mu=\frac{c}{b}\right). \tag{11}$$

The functions $f_{i/A}$ and $f_{j/B}$ are the modified parton distributions [6,12],

$$f_{i/A}(x_A,\mu) = \sum_a \int_{x_A}^1 \frac{d\xi}{\xi}C_{i/a}\left(\frac{x_A}{\xi},\mu\right)\phi_{a/A}(\xi,\mu) \tag{12}$$

where Σ_a runs over all parton flavors. In Eq. (12), $\phi_{a/A}(\xi,\mu)$ is the normal parton distribution for finding a parton of flavor a in hadron A, and $C_{i/a} = \Sigma_{n=0}C_{i/a}^{(n)}(\alpha_s/\pi)^n$ are perturbatively calculable coefficient functions for finding a parton i from a parton a. The first two coefficients of $C_{i/a}$ are available [6,9]:

$$C_{i/j}^{(0)}(z,\mu=c/b) = \delta_{ij}\delta(z-1),$$

$$C_{i/g}^{(0)}(z,\mu=c/b) = 0,$$

$$C_{i/j}^{(1)}(z,\mu=c/b)=\delta_{ij}\frac{C_F}{2}\Bigg[(1-z)+\left(\frac{\pi^2}{2}-4\right)\delta(1-z)\Bigg],$$

$$C_{i/g}^{(1)}(z,\mu=c/b)=T_R z(1-z) \tag{13}$$

where i and j represent quark or antiquark flavors and g represents a gluon. The coefficient functions given in Eq. (13) are derived from the general functional forms in Ref. [6] by setting the renormalization constants and the factorization scale as $C_1=c$, $C_2=1$, and $\mu=c/b$.

The $\sigma_{ij\to V}(Q)$ in Eq. (2) is the lowest order cross section for a pair of quark and antiquark to annihilate into a vector boson ($V=\gamma^*$, $W^{\pm}$, or Z). For $V=\gamma^*$, we have

$$\sigma_{ij\to\gamma^*}(Q)=\delta_{j\bar{i}}e_i^2\left(\frac{4\pi^2\alpha_{EM}^2}{3S}\right)\frac{1}{N}\frac{1}{Q^2} \tag{14}$$

where e_i is the quark fractional charge and $N=3$ for SU(3) color. The $\sigma_{ij\to V}(Q)$ for $V=W^{\pm}$ or Z can be found in Refs. [6,12].

In the CSS resummation formalism, the Y term in Eq. (1) represents a small correction to the Q_T distribution when $Q_T\ll Q$. But it dominates the Q_T distributions when $Q_T\sim Q$. The Y term has a perturbative expansion, $Y=\Sigma_{n=1}Y^{(n)}(\alpha_s(\mu)/\pi)^n$, and the coefficients $Y^{(n)}$ have the following factorized form [6]:

$$Y^{(n)}(Q_T,Q,x_A,x_B;\mu)=\sum_{a,b}\int_{x_A}^1\frac{d\xi_A}{\xi_A}\phi_{a/A}(\xi_A,\mu)\int_{x_B}^1\frac{d\xi_B}{\xi_B}\phi_{b/B}(\xi_B,\mu)\times\left(\frac{4\pi^2\alpha_{EM}^2}{9Q^2S}\right)R_{ab\to V}^{(n)}(Q_T,Q,x_A/\xi_A,x_B/\xi_B;\mu), \tag{15}$$

where $\Sigma_{a,b}$ run over all possible parton flavors and μ represents both the factorization and renormalization scale. The $R_{ab\to V}^{(n)}$ in Eq. (15) are perturbatively calculable and have the same normalization as those introduced in Ref. [6]. The leading order terms $R_{ab\to\gamma^*}^{(1)}$ are available and are given by Eqs. (2.9)–(2.12) in Ref. [6]. For $W^{\pm}$ and Z production, one needs to change the fractional quark charge e_i^2 in the $R_{ab\to\gamma^*}^{(1)}$ by corresponding weak coupling constants [6].

Since the Y term does not have large logarithms and is perturbatively calculable, the predictive power of the CSS formalism relies on our ability to predict the $\tilde{W}$ term in Eq. (1). Because the leading power perturbative QCD calculations and the normal parton distributions in Eq. (12) are only valid for $\mu>\mu_0\sim 1$–2 GeV, the perturbatively calculated b-space distribution $\tilde{W}(b,Q,x_A,x_B)$ in Eq. (1) is reliable only if the momentum scale $1/b>\mu_0$. On the other hand, the Fourier transform in Eq. (1) requires a b-space distribution $\tilde{W}(b,Q,x_A,x_B)$ for $b\in[0,\infty)$. Therefore, the predictive power of the b-space resummation formalism is limited by our inability to calculate the nonperturbative b-space distribution at large b [1,14].

However, the b-space resummation formalism has a remarkable feature that the resummed exponential factor $\exp[-S(b,Q)]$ suppresses the b integral when b is larger than $1/Q$. Therefore, when $Q\gg\mu_0$, it is possible that the Fourier transform in Eq. (1) is dominated by a region of b much smaller than $1/\mu_0$, and the calculated Q_T distributions are insensitive to the nonperturbative information at large b. In fact, using the saddle point method, it was shown [4,6] that for a large enough Q, the QCD perturbation theory is valid even at $Q_T=0$, and the Fourier transform in Eq. (1) is dominated by an impact parameter of order

$$b_{\rm SP}=\frac{1}{\Lambda_{\rm QCD}}\left(\frac{\Lambda_{\rm QCD}}{Q}\right)^{\lambda} \tag{16}$$

where $\lambda=16/(49-2n_f)\approx 0.41$ for quark flavors $n_f=5$. From Eq. (16), the momentum scale corresponding to the saddle point, $1/b_{\rm SP}$, can be well within the perturbative region if the value of Q is large enough. Therefore, the predictive power of the b-space resummation formalism is directly related to the numerical value of the vector boson's invariant mass Q [4,6].

For $W^{\pm}$ and Z production, we have $Q\sim M_W$ or M_Z and the corresponding momentum scale from Eq. (16), $1/b_{\rm SP}\approx 10\Lambda_{\rm QCD}\sim 2$ GeV, which is at the borderline of the predictive power of perturbative QCD calculations without introducing the power corrections. In the rest of this section, we show that the next-to-leading order corrections to the function $S(b,Q)$ reduce the numerical value of the $b_{\rm SP}$. Furthermore, we show that the numerical value for the saddle point has a strong dependence on the collision energy $\sqrt{S}$, and the $\sqrt{S}$ dependence can either improve or reduce the predictive power of the b-space resummation formalism.

Since there is no preferred transverse direction, $\tilde{W}$ in Eq. (1) is a function of $b=|\vec{b}|$, and the Fourier transform can be written as

$$\frac{1}{(2\pi)^2}\int d^2b e^{i\vec{Q}_T\cdot\vec{b}}\tilde{W}(b,Q,x_A,x_B)=\frac{1}{2\pi}\int_0^\infty dbbJ_0(Q_Tb)e^{-S(b,Q)}\times\sum_{ij}\sigma_{ij\to V}(Q)\tilde{W}_{ij}\left(b,\frac{c}{b},x_A,x_B\right), \tag{17}$$

where $J_0(z)$ with $z=Q_Tb$ is the Bessel function. In deriving Eq. (17), we used Eqs. (2) and (3). The $b_{\rm SP}$ in Eq. (16) was derived by solving

$$\frac{d}{db}\ln(be^{-S(b,Q)})_{b=b_{\rm SP}}=0 \tag{18}$$

with only $A^{(1)}$ for the function $S(b,Q)$. Solving Eq. (18) for the saddle point relies on the assumption that the b dependence in $\tilde{W}_{ij}(b,c/b,x_A,x_B)$ is smooth around $b_{\rm SP}$.

However, we find from Eq. (11) that the b dependence in $\tilde{W}_{ij}(b,c/b,x_A,x_B)$ is strongly connected to the numerical values of x_A and x_B, and can be very important for determining the saddle point if x_A and x_B are very small or very large [8]. Taking into account the full b dependence of $\tilde{W}_{ij}(b,c/b,x_A,x_B)$, the saddle point for the b integration in Eq. (17) at $Q_T=0$ is determined by solving the following equation:

$$\frac{d}{db}\ln(b\mathrm{e}^{-S(b,Q)})_{b=b_0} + \frac{d}{db}\ln\left[\sum_{ij}\ \sigma_{ij\to V}(Q)\tilde{W}_{ij}\left(b,\frac{c}{b},x_A,x_B\right)\right]_{b=b_0}=0. \tag{19}$$

If the $\tilde{W}_{ij}(b,c/b,x_A,x_B)$ has a weak b dependence around b_0, the second term in Eq. (19) can be neglected, and the $b_0\approx b_{\rm SP}$. From Eq. (11), the b dependence of $\tilde{W}_{ij}(b,c/b,x_A,x_B)$ is directly proportional to the evolution of the modified parton distributions:

$$\frac{d}{db}\ln\left[\sum_{ij}\ \sigma_{ij\to V}(Q)\tilde{W}_{ij}\left(b,\frac{c}{b},x_A,x_B\right)\right] \propto -\frac{1}{b}\left[\frac{d}{d\ln\mu}f_{i/A}(x_A,\mu)\ \text{ or }\ \frac{d}{d\ln\mu}f_{j/B}(x_B,\mu)\right], \tag{20}$$

where $\mu=c/b$. Since the coefficient functions C in Eq. (13) do not have a b dependence at these orders, the evolution of the modified parton distributions in Eq. (20) is directly proportional to the evolution of normal parton distributions, $(d/d\ln\mu)\phi_{i/A}(\xi,\mu)$. Because of the steep falling feature of the normal parton distributions when ξ increases, the convolution over ξ in Eq. (12) is dominated by the value of $\xi\sim x_A$. Therefore, the evolution of the modified parton distributions in Eq. (20) is directly proportional to the evolution of normal parton distributions, $(d/d\ln\mu)\phi_{i/A}(\xi,\mu)$ at $\xi\sim x_A$. From the Dokshitzer-Gribov-Lipatov-Altarelli-Pariai (DGLAP) equation, it is known that $(d/d\ln\mu)\phi(x,\mu)$ is positive (or negative) for $x<x_0\sim 0.1$ (or $x>x_0$), and the evolution is very steep when x is far away from x_0. Therefore, the second term in Eq. (19) should be very important when x_A and x_B are much smaller than the x_0.

Since Eq. (18) has a saddle point solution, the first term in Eq. (19) is a decreasing function of b, and it vanishes at $b=b_{\rm SP}$. Because of the minus sign in Eq. (20) and the fact that the number of small x partons increases when the scale μ increases, we expect the second term in Eq. (19) to be negative when x_A and x_B are smaller than the typical x_0, and to reduce the numerical value of the saddle point. As a demonstration, let $Q=6$ GeV and $\sqrt{S}=1.8$ TeV. Using CTEQ4M parton distributions and $\Lambda_{\rm QCD}(n_f=5)=0.202$ GeV [15], one derives from Eq. (16) that $b_{\rm SP}\approx 1.2\ \mathrm{GeV}^{-1}$, and might conclude that the perturbatively resummed Q_T distribution at the given values of Q and $\sqrt{S}$ is not reliable. However, as shown in Fig. 1(a), the integrand of the b integration in Eq. (17) has a nice saddle point at $b_0\approx 0.38\ \mathrm{GeV}^{-1}$, which is within the perturbative region. This is due to the fact that $x_A\sim x_B\sim 0.003$ are very small. The second terms in Eq. (19) is negative and it reduces the numerical value of the saddle point, which is clearly shown in Fig. 1(b). The solid line and dashed line represent the first and the second term in Eq. (19), respectively. Although the solid line in Fig. 1(b) never crosses zero for $b<1\ \mathrm{GeV}^{-1}$, which is consistent with the fact that $b_{\rm SP}\sim 1.2\ \mathrm{GeV}^{-1}$, the dashed line is negative and it cancels the solid line to give a nice saddle point at $b=b_0\sim 0.38\ \mathrm{GeV}^{-1}$.

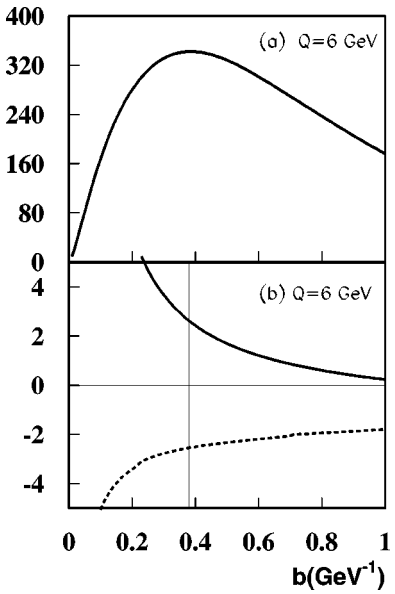

FIG. 1. (a) Integrand of the b integration in Eq. (17) at $Q_T=0$ and $Q=6$ GeV as a function of b with an arbitrary normalization at Tevatron energy; (b) the first (solid line) and second (dashed line) terms in Eq. (19) as a function of b at the same Q and $\sqrt{S}$.

Similar to Fig. 1, we plot the integrand of the b integration in Eq. (17) for Z production at Tevatron and the LHC energies in Figs. 2 and 3, respectively. In plotting both figures, we used CTEQ4M parton distributions and the perturbatively calculated functions A, B, and C to the next-to-leading order, which are listed in Eqs. (9) and (13). From Eq. (16), we estimate $b_{\rm SP}\approx 0.4\ \mathrm{GeV}^{-1}$ for $Q=M_Z$. As shown in Fig. 2(b), the solid line vanishes at $b\approx 0.27\ \mathrm{GeV}^{-1}$, which indicates that the inclusion of $A^{(2)}$, $B^{(1)}$, and $B^{(2)}$ reduces the numerical value of the saddle point, $b_{\rm SP}$. The dashed line in Fig. 2(b), which corresponds to the second term in Eq. (19), further reduces the numerical value of the saddle point to $b_0\approx 0.24\ \mathrm{GeV}^{-1}$. At the LHC energy, x_A and x_B are much smaller. We then expect the second term in Eq. (19) to be more important, which is clearly shown in Fig. 3(b). The dashed line in Fig. 3(b) has a much larger absolute value in comparison with that in Fig. 2(b). Consequently, the numerical value of the saddle point is further reduced from $b_0\approx 0.24\ \mathrm{GeV}^{-1}$ at $\sqrt{S}=1.8$ TeV to $b_0\approx 0.13\ \mathrm{GeV}^{-1}$ at

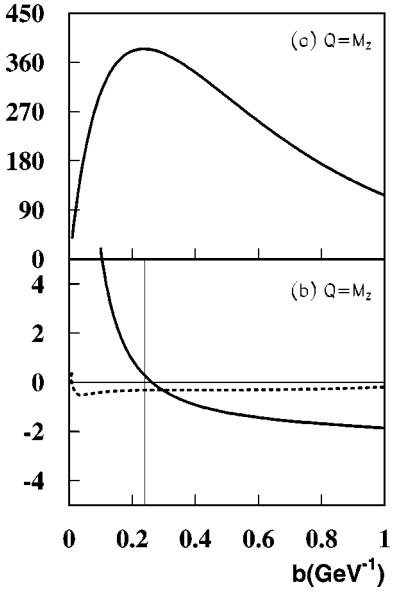

FIG. 2. (a) Integrand of the b integration in Eq. (17) at $Q_T=0$ and $Q=M_Z$ as a function of b with an arbitrary normalization at Tevatron energy ($\sqrt{S}=1.8$ TeV); (b) the first (solid line) and second (dashed line) terms in Eq. (19) as a function of b at the same Q and $\sqrt{S}$.

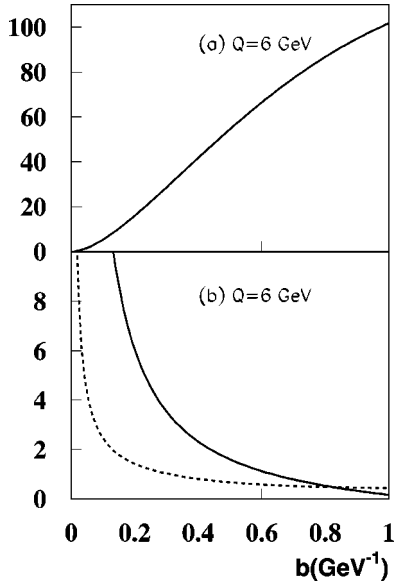

FIG. 4. (a) Integrand of the b integration in Eq. (17) at $Q_T=0$ and $Q=6$ GeV as a function of b with an arbitrary normalization at E288 energy ($\sqrt{S}=27.4$ GeV); (b) the first (solid line) and second (dashed line) terms in Eq. (19) as a function of b at the same Q and $\sqrt{S}$.

$\sqrt{S}=14$ TeV, where the perturbative QCD calculations should be reliable. In addition, the narrow width of the b distribution shown in Fig. 3(a) ensures that the b integration is dominated by $b\sim b_0$. In conclusion, even at $Q_T=0$, the perturbative QCD based b-space resummation formalism is valid as long as the collision energy $\sqrt{S}$ is large enough.

When $Q_T>0$, the Bessel function $J_0(z=Q_Tb)$ further suppresses the large b region of the b integration. Because the argument of the Bessel function is proportional to Q_T, the large b region is more suppressed if Q_T is larger. That is, the larger Q_T is, the better the b-space resummation formalism is expected to work. However, it has been known [1] that the b-space resummed Q_T distribution from Eq. (1) becomes unphysical or even negative when Q_T is large. For example, a matching between the resummed and fixed-order calculations has to take place at $Q_T\sim 50$ GeV for $W^{\pm}$ production when these two predictions cross over [14]. We will address this puzzle in Sec. IV.

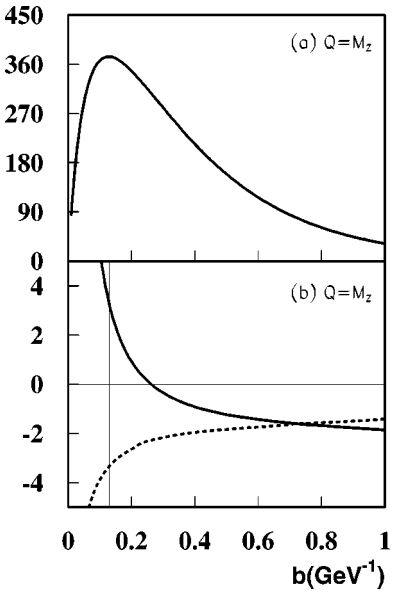

FIG. 3. (a) Integrand of the b integration in Eq. (17) at $Q_T=0$ and $Q=M_Z$ as a function of b with an arbitrary normalization at the LHC energy ($\sqrt{S}=14$ TeV); (b) the first (solid line) and second (dashed line) terms in Eq. (19) as a function of b at the same Q and $\sqrt{S}$.

In the rest of this section, we investigate the predictive power of the b-space resummation formalism for the Drell-Yan production at fixed target energies ($\sqrt{S}\leqslant 40$ GeV). Most data at the fixed target energies have $Q\in(5,12)$ GeV and Q_T at a few GeV or less. From Eq. (16), we find that $b_{\rm SP}$ is of order 1 GeV^{-1} or larger. Because of the low collision energy, the typical values of x_A and x_B are larger than the x_0. Therefore, the second term in Eq. (19) should be positive, which increases the numerical value of the saddle point. As an illustration, instead of $\sqrt{S}=1.8$ TeV, we replot all quantities in Fig. 1 at $\sqrt{S}=27.4$ GeV in Fig. 4, which is the collision energy for Fermilab experiment E288 [16]. As expected, the dashed line is now positive and the saddle point is no longer in the perturbative region. In conclusion, at fixed target energies, the perturbatively calculated b-space distribution derived from the CSS resummation formalism is not sufficient to predict the Drell-Yan Q_T distributions at $Q_T=0$. A nonperturbative extrapolation to the large b region is necessary.

When $Q_T>0$, the Bessel function $J_0(z=Q_Tb)$ suppresses the large b region of the b integration, and improves the predictive power of the b-space resummation formalism at the fixed target energies. In Fig. 5, we plot the integrand of

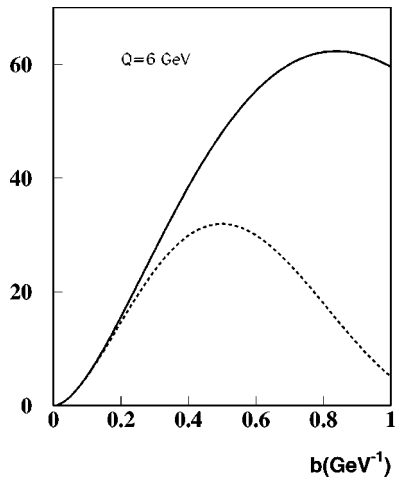

FIG. 5. Integrand of the b integration in Eq. (17) at $Q_T=1$ GeV (solid line) and $Q_T=2$ GeV (dashed line) as a function of b with an arbitrary normalization. The Q and $\sqrt{S}$ are the same as those in Fig. 4(a).

the b integration in Eq. (17) at $Q_T=1$ GeV (solid line) and $Q_T=2$ GeV (dashed line) for $Q=6$ GeV and $\sqrt{S}=27.4$ GeV. As shown in Fig. 5, the saddle point for the b-integration moves to the smaller b region as Q_T increases. Since the saddle points of both curves in Fig. 5 are within the perturbative region, one might expect the b-space resummation formalism to provide a good description of the Q_T distributions at these energies. However, as a result of the oscillatory nature of the Bessel function, the precise value of the b integration depends on the detailed cancellations in the large b region. Therefore, the predictive power of the b-space resummation formalism at the fixed target energies is still limited by our knowledge of the nonperturbative information at large b. More discussions are given in Sec. IV.

III. EXTRAPOLATION TO THE LARGE b REGION

In this section, we quantitatively analyze the role of the nonperturbative input at large b in the b-space resummation formalism. We first briefly review the extrapolation defined in Eq. (4) and its status in comparison with the existing data. Then, by adding possible power corrections to the renormalization group equations in Eqs. (6) and (7), we derive a new functional form for extrapolating the perturbatively resummed $\tilde{W}(b,Q,x_A,x_B)$ to the large b region. This new functional form clearly separates the perturbative prediction at small b from the nonperturbative physics in the large b region.

A. Extrapolation proposed by Collins, Soper, and Sterman

As discussed in last section, the perturbatively resummed $\tilde{W}(b,Q,x_A,x_B)$ in Eq. (2) is only reliable for the small b region. An extrapolation of the perturbatively calculated $\tilde{W}(b,Q,x_A,x_B)$ to the large b region is necessary in order to complete the Fourier transform in Eq. (1). In Ref. [6], CSS proposed the following extrapolation:

$$\tilde{W}^{\rm CSS}(b,Q,x_A,x_B)\equiv\sum_{ij}\ \sigma_{ij\to V}(Q)\tilde{W}_{ij}(b_*,Q,x_A,x_B)\times F_{ij}^{NP}(b,Q,x_A,x_B), \tag{21}$$

where b_* was defined following Eq. (4), and the perturbatively calculated $\tilde{W}_{ij}(b,Q,x_A,x_B)$ are given in Eq. (3). The nonperturbative input distributions F_{ij}^{NP} have the following functional form [6]:

$$F_{ij}^{NP}(b,Q,x_A,x_B)=\exp[-\ln(Q^2/Q_0^2)g_1(b)-g_{i/A}(x_A,b)-g_{j/B}(x_B,b)] \tag{22}$$

where the $\ln(Q^2)$ dependence is a derived result. The functions $g_1(b)$, $g_{i/A}(x_A,b)$, and $g_{j/B}(x_B,b)$ are nonperturbative, and should go to zero as $b\to 0$. The predictive power of the CSS formalism relies on the derived Q^2 dependence and the universality of the F_{ij}^{NP}. Since the low energy Drell-Yan data are sensitive to the large b region, in principle, one can use the low Q^2 data to fix the parameters of the nonperturbative F_{ij}^{NP} and predict the Q_T distributions of $W^{\pm}$ and Z production at high Q^2.

Davis, Webber, and Stirling (DWS) introduced the following form for the nonperturbative distribution F_{ij}^{NP} [9]:

$$F_{DWS}^{NP}(b,Q,x_A,x_B)=\exp\{-b^2[g_1+g_2\ln(Q/2Q_0)]\}, \tag{23}$$

where $Q_0=2$ GeV$=1/b_{max}$, and g_1 and g_2 are flavor independent fitting parameters. Without the flavor dependence, the extrapolated CSS formalism defined in Eq. (21) reduces to that in Eq. (4). With $g_1=0.15$ GeV^2 and $g_2=0.4$ GeV^2, DWS found [9] that the CSS b-space resummation formalism gives a reasonable description of the Drell-Yan data from Fermilab experiment E288 at $\sqrt{S}=27.4$ GeV [16] as well as CERN Intersecting Storage Rings (ISR) experiment R209 at $\sqrt{S}=62$ GeV [17].

In order to incorporate possible $\ln(\tau)$ dependence with $\tau=Q^2/S=x_Ax_B$, Ladinsky and Yuan (LY) proposed a modified functional form for F_{ij}^{NP} [11]:

$$F_{LY}^{NP}(b,Q,x_A,x_B)=\exp\{-b^2[g_1+g_2\ln(Q/2Q_0)]-bg_1g_3\ln(100x_Ax_B)\}. \tag{24}$$

An extra parameter g_3 was introduced in the LY parametrization of the nonperturbative F_{ij}^{NP}. Similar to the DWS parametrization, no flavor dependence was introduced into the nonperturbative distribution. With $g_1=0.11^{+0.04}_{-0.03}$ GeV^2, $g_2=0.58^{+0.1}_{-0.2}$ GeV^2, and $g_3=-0.15^{+0.1}_{-0.1}$ GeV^{-1}, LY were able to fit the R209 Drell-Yan data as well as CDF data on W and Z production from Fermilab. More recently, Landry, Brock, Ladinsky, and Yuan (LBLY) performed a much more extensive global fit to the low energy Drell-Yan data as well as high energy W and Z data by using both DWS and LY parametrizations [13]. In order to fit both the low energy Drell-Yan and the collider W and Z data, LBLY found that it is necessary to introduce a large overall normalization uncertainty in order to include the low energy Drell-Yan data (in

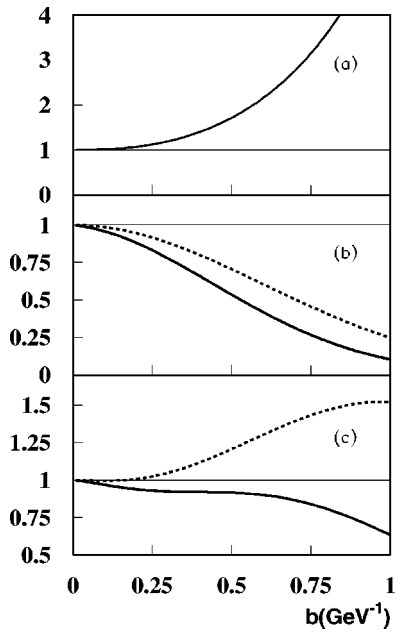

FIG. 6. (a) ratio $\tilde{W}(b_*,Q,x_A,x_B)/\tilde{W}(b,Q,x_A,x_B)$ as a function of b; (b) $F^{NP}(b,Q,x_A,x_B)$ as a function of b; (c) Ratio R_W defined in Eq. (25) as a function of b. All plots have $Q=M_Z$ and $\sqrt{S}=1.8$ TeV.

particular, E288 data) into the global fit [13]. LBLY also emphasized that the collider data on Z production are very useful in determining the value of fitting parameter g_2. They concluded [13] that both DWS and LY parametrizations with updated parameters result in good global fits, but give measurable differences in Q_T distributions of Z production at the Fermilab Tevatron.

Based on our discussions in last section, the Q_T distributions of Z production at collider energies should not be very sensitive to the nonperturbative physics from the large b region. Any significant dependence on the fitting parameters for Z production would cast a doubt on the predictive power of the b-space resummation formalism. To understand the fitting parameter dependence of the Z production, we introduce the following ratio:

$$R_W(b,Q,x_A,x_B)\equiv\frac{\tilde{W}^{\rm CSS}(b,Q,x_A,x_B)}{\tilde{W}(b,Q,x_A,x_B)} =\frac{\tilde{W}(b_*,Q,x_A,x_B)}{\tilde{W}(b,Q,x_A,x_B)}F^{NP}(b,Q,x_A,x_B), \tag{25}$$

where $\tilde{W}(b,Q,x_A,x_B)$ is the perturbatively calculated b-space distribution given in Eq. (2). In deriving the second line in Eq. (25), we used the fact that both DWS and LY parametrizations of the F^{NP} are independent of the parton flavors. Using CTEQ4M parton distributions, we plot in Fig. 6(a) the ratio $\tilde{W}(b_*,Q,x_A,x_B)/\tilde{W}(b,Q,x_A,x_B)$ as a function of b at $Q=M_Z$ and $\sqrt{S}=1.8$ TeV. In Fig. 6(b), we plot the nonperturbative distribution $F^{NP}(b,Q,x_A,x_B)$ as a function of b with both DWS parameters (dashed line) and LY parameters (solid line). In Fig. 6(c), we plot the ratio $R_W(b,Q,x_A,x_B)$ defined in Eq. (25), which is effectively equal to a product of Fig. 6(a) and Fig. 6(b). From Fig. 6, we learn that the introduction of the b_* significantly changes the perturbatively calculated b-space distribution within the perturbative region, and in the same region, the function F^{NP} can deviate from unity by as much as 50% percents for some fitting parameters. In order to preserve the predictive power of the perturbative calculations, it is important to keep $\tilde{W}^{\rm CSS}(b,Q,x_A,x_B)$ consistent with the perturbatively calculated $\tilde{W}(b,Q,x_A,x_B)$ when $b<b_{max}$ [or $R_W(b,Q,x_A,x_B)\approx 1$]. However, we find that a significant fitting parameter dependence (as much as 20%) was introduced by $\tilde{W}^{\rm CSS}(b,Q,x_A,x_B)$ to the b-space distribution within the perturbative region. The same conclusion holds if we plot the curves at different energies or use other sets of fitting parameters available for the F^{NP} [12,13].

B. Extrapolation with dynamical power corrections

In order to separate the perturbative prediction in the small b region from the nonperturbative physics at large b, we derive a new functional form to extrapolate the perturbatively calculated $\tilde{W}(b,Q,x_A,x_B)$ to the large b region. Our goal is to have an extrapolation that preserves the predictive power of perturbative calculations in the small b region and extends to the large b region with as much correct physics as we can put in.

Taking advantage of our early conclusion that heavy boson production at collider energies should not be very sensitive to the large b region, we can improve the leading power perturbative QCD calculations by studying the behavior of power corrections in the region of b space where b is not too much larger than b_{max}. The power correction in QCD is a very rich and difficult subject itself [18–21]. In order to define the power corrections, we have to identify a nonperturbative momentum scale, Λ, which should be of order $\Lambda_{\rm QCD}$. For example, the nonperturbative scale can be the target mass [22] or matrix elements of high twist operators [18–20]. In addition, we have to distinguish two different types of power corrections: (1) the power corrections directly to the physical observables (such as cross sections or structure functions) and (2) the power corrections to the evolution or renormalization group equations. The type-1 (or direct) power corrections are always proportional to the power of (Λ/Q) with the physically observed momentum scale Q [18–20]. Therefore, the effect of this type of power corrections to physical observables can be neglected when $(\Lambda/Q)\to 0$. Similarly, the type-2 (or indirect) power corrections are proportional to the power of (Λ/μ) with evolution or renormalization scale μ. It is important to note that physical observables are not directly proportional to the evolution or renormalization group equations; instead, they depend on the *solutions* of these equations. Therefore, physical observables carry the effect of type-2 power corrections for all $\mu\in[Q_0,Q]$ and the boundary conditions at the scale Q_0 [23]. Even when Q is much larger than Λ, physical observables

can still carry a large effect of the type-2 power corrections through the evolution from Q_0 to Q [24]. In this subsection, we concentrate on the type-2 power corrections. Because they contribute to the evolution or renormalization group equations, these power corrections should have a dynamical origin.

When $b>b_{max}$, we solve the evolution equation in Eq. (5) from $\ln(c^2/b_{max}^2)$ to $\ln(Q^2)$ in order to separate the leading power QCD calculations at small b from the large b region. Because the scale Q of the evolution equation is chosen to be larger than c/b_{max}, we can ignore the explicit $1/Q^2$ power corrections to this equation.

However, the kernel $K(b\mu,\alpha_s(\mu))$ of the evolution equation has an explicit b dependence; we need to add power corrections to its renormalization group equation when $b>b_{max}$. Similarly, we need to add power corrections to the renormalization group equation of the kernel $G(Q/\mu,\alpha_s(\mu))$ when $1/\mu>b_{max}$. Since we are only interested in deriving a functional form of the b dependence due to power corrections, we will not attempt to derive the exact coefficients of the power corrections to the renormalization group equations by going through a detailed analysis of the mixing of leading and high twist operators [23]. Instead, we introduce some fitting parameters for the size of the possible power corrections. For including only the leading power corrections, we modify the renormalization group equations in Eqs. (6) and (7) as follows:

$$\frac{\partial}{\partial \ln \mu^2} K(b\mu,\alpha_s(\mu)) = -\frac{1}{2}\gamma_K(\alpha_s(\mu)) - \frac{1}{\mu^2}\overline{\gamma}_K, \quad (26)$$

$$\frac{\partial}{\partial \ln \mu^2} G(Q/\mu,\alpha_s(\mu)) = \frac{1}{2}\gamma_K(\alpha_s(\mu)) + \frac{1}{\mu^2}\overline{\gamma}_K, \quad (27)$$

where $\overline{\gamma}_K$ is treated as an unknown parameter here, though it should in principle depend on $\alpha_s(\mu)$ and the characteristic size of high twist operators. In Eqs. (26) and (27), we parametrize the leading power corrections in such a way that they preserve $(d/d\ln\mu^2)\tilde{W}_{ij}(b,Q,x_A,x_B)=0$. Since we are interested in the region of b not too much larger than b_{max}, we neglect higher power corrections in Eqs. (26) and (27). This approximation is going to be tested in Sec. IV.

By integrating Eq. (26) over $\ln(\mu^2)$ from $\ln(c^2/b^2)$ to $\ln(\mu^2)$ and Eq. (27) from $\ln(Q^2)$ to $\ln(\mu^2)$, we have

$$\begin{aligned} &K(b\mu,\alpha_s(\mu)) + G(Q/\mu,\alpha_s(\mu)) \\ &\approx -\int_{c^2/b_{max}^2}^{Q^2} \frac{d\bar{\mu}^2}{\bar{\mu}^2} A(\alpha_s(\bar{\mu})) - B(\alpha_s(Q)) \\ &\quad - \int_{c^2/b^2}^{c^2/b_{max}^2} \frac{d\bar{\mu}^2}{\bar{\mu}^2}\left[\frac{1}{2}\gamma_K(\alpha_s(\bar{\mu})) + \frac{1}{\bar{\mu}^2}\overline{\gamma}_K\right] \\ &\quad + \left[K\left(c,\alpha_s\left(\frac{c}{b}\right)\right) - K\left(c,\alpha_s\left(\frac{c}{b_{max}}\right)\right)\right], \end{aligned} \quad (28)$$

where A and B are the same as those defined in Eq. (8). In deriving Eq. (28), we neglected the power corrections for the momentum scale between c^2/b_{max}^2 and Q^2, which is consistent with neglecting the $1/Q^2$ term in the evolution equation of the $\tilde{W}_{ij}(b,Q,x_A,x_B)$. Substituting the K and G in Eq. (28) into the evolution equation in Eq. (5) and solving the evolution equation over the $\ln(Q^2)$ from $\ln(c^2/b_{max}^2)$ to $\ln(Q^2)$, we obtain the solution for $b>b_{max}$:

$$\begin{aligned} \tilde{W}_{ij}^{QZ}(b,Q,x_A,x_B) &= \tilde{W}_{ij}(b_{max},Q,x_A,x_B) \\ &\quad \times \tilde{F}_{ij}^{NP}(b,Q,x_A,x_B;b_{max}) \end{aligned} \quad (29)$$

where $\tilde{W}_{ij}$ is the leading power perturbative solution given in Eq. (3), and

$$\begin{aligned} &\tilde{F}_{ij}^{NP}(b,Q,x_A,x_B;b_{max}) \\ &= \frac{\tilde{W}_{ij}(b,c/b_{max},x_A,x_B)}{\tilde{W}_{ij}(b_{max},c/b_{max},x_A,x_B)} \exp\left(-\ln\left(\frac{Q^2 b_{max}^2}{c^2}\right)\right. \\ &\quad \times \left\{ \frac{\gamma}{\alpha}[(b^2)^\alpha - (b_{max}^2)^\alpha] + \frac{\overline{\gamma}_K}{c^2}(b^2 - b_{max}^2)\right. \\ &\quad \left.\left. - \left[K\left(c,\alpha_s\left(\frac{c}{b}\right)\right) - K\left(c,\alpha_s\left(\frac{c}{b_{max}}\right)\right)\right]\right\}\right). \end{aligned} \quad (30)$$

The nonperturbative function $\tilde{F}_{ij}^{NP}\to 1$ as $b\to b_{max}$. In deriving Eq. (30), we approximate the μ dependence of $\gamma_K(\alpha_s(\mu))$ in the small μ region by $\frac{1}{2}\gamma_K(\alpha_s(\mu)) \approx \gamma(\mu^2)^{-\alpha}$ with constant parameters γ and α, and we expect α to be much less than 1. This approximation is to mimic a summation of a perturbative series in powers of the running coupling constant, $(\alpha_s(\mu))^m$, with the scale μ extrapolated into the nonperturbative region [25]. Since $[K(c,\alpha_s(c/b)) - K(c,\alpha_s(c/b_{max}))]$ in Eq. (30) depends only on b and b_{max} through α_s, we can combine it with the first term and treat the power α and the coefficient as fitting parameters. Since the b dependence of $\tilde{W}_{ij}(b,c/b_{max},x_A,x_B)$ depends on the evolution of parton distributions, $\ln[\tilde{W}_{ij}(b,c/b_{max},x_A,x_B)/\tilde{W}_{ij}(b_{max},c/b_{max},x_A,x_B)]$ changes sign when x_A and x_B are larger or smaller than the typical x_0. Therefore, we can parametrize the ratio

$$\begin{aligned} &\frac{\tilde{W}_{ij}(b,c/b_{max},x_A,x_B)}{\tilde{W}_{ij}(b_{max},c/b_{max},x_A,x_B)} \\ &\quad \approx \exp\left\{ g_3 \ln\left(\frac{x_A x_B}{x_0^2}\right)[(b^2)^\beta - (b_{max}^2)^\beta]\right\} \end{aligned} \quad (31)$$

with parameters g_3 and β. In principle, the parameters g_3 and β as well as x_0 can depend on parton flavors because of the flavor dependence of parton evolutions. Since parton distributions are near saturation at a very small momentum scale [26], we expect both g_3 and β to be very small, and therefore, this term can be neglected in comparison with other terms in the $\tilde{F}_{ij}^{NP}$. Consequently, we can neglect the

flavor dependence of the $\tilde{F}_{ij}^{NP}$. In conclusion, without losing the characteristic features of the b dependence in Eq. (30), we can reparametrize $\tilde{F}_{ij}^{NP}$ as

$$\tilde{F}_{QZ}^{NP}(b,Q,x_A,x_B;b_{max}) = \exp\left\{ -\ln\left(\frac{Q^2 b_{max}^2}{c^2}\right) \times \{g_1[(b^2)^\alpha - (b_{max}^2)^\alpha] + g_2(b^2 - b_{max}^2)\}\right\} \tag{32}$$

where the explicit $\ln(Q^2 b_{max}^2/c^2)$ dependence is derived from the evolution equation in Eq. (5). In Eq. (32), the b^2 term represents the leading power corrections to the renormalization group equations of the kernels K and G, and the $(b^2)^\alpha$ term is a consequence of extrapolating the leading power part of the kernels K and G to the small momentum scale $1/b$ with all powers of running coupling constants resummed [25]. The actual size of g_2 signals the size of dynamical power corrections. The choices for the parameters g_1 g_2, and $\alpha < 1$, will be discussed in Sec. IV.

We summarize this subsection by writing down our derived extrapolation [8]:

$$\tilde{W}^{QZ}(b,Q,x_A,x_B) = \begin{cases} \tilde{W}(b,Q,x_A,x_B), & b \leqslant b_{max}, \\ \tilde{W}(b_{max},Q,x_A,x_B)\tilde{F}_{QZ}^{NP}(b,Q,x_A,x_B;b_{max}), & b > b_{max}, \end{cases} \tag{33}$$

with $\tilde{W}(b,Q,x_A,x_B)$ given in Eq. (2), and the function $\tilde{F}_{QZ}^{NP}$ specified in Eq. (32). Since the evolution equation in Eq. (5) and the renormalization group equations in Eqs. (6) and (7) do not include any power corrections, the solution of these equations, $\tilde{W}(b,Q,x_A,x_B)$ in Eq. (33), is valid only for $b < b_c$ with $b_c \sim 0.75\ \text{GeV}^{-1}$, which was estimated by setting $\ln(1/b_c^2) \sim b_c^2$. Therefore, the numerical value of b_{max} in Eq. (33) should not be larger than b_c in order to be consistent with the approximation used to derive $\tilde{W}(b,Q,x_A,x_B)$.

C. Corrections from the parton intrinsic transverse momentum

In Eq. (32), all b dependence in F_{QZ}^{NP} is dynamical in nature from the way we solve the evolution and renormalization group equations. We show in this subsection that there could be corrections from the Q-independent intrinsic b dependence to the b-space distribution $\tilde{W}^{QZ}(b,Q,x_A,x_B)$ in Eq. (33).

For an arbitrary function $F(b)$, we introduce

$$W_{ij}(b,Q,x_A,x_B) \equiv F(b)\tilde{W}_{ij}(b,Q,x_A,x_B), \tag{34}$$

and find that both $W_{ij}(b,Q,x_A,x_B)$ and $\tilde{W}_{ij}(b,Q,x_A,x_B)$ can be solutions of the same evolution equation in Eq. (5). In principle, the function $F(b)$ can also have a dependence on parton flavors i and j. If we use the $W_{ij}(b,Q,x_A,x_B)$ instead of $\tilde{W}_{ij}(b,Q,x_A,x_B)$ as our solution for the QCD resummed b-space distribution in Eq. (2), the function $F(b)$ should be very close to 1 when b is small ($< b_{max}$). Otherwise, its inclusion will not be consistent with the leading power QCD calculation because the dominant physics in the small b region has been included in the perturbatively calculated $\tilde{W}_{ij}(b,Q,x_A,x_B)$. But when b is larger than b_{max}, neither the evolution equation nor the renormalization group equations have any constraints on the functional form of the $F(b)$, as long as it is not a function of Q.

Physically, however, we do not have an arbitrary function $F(b)$. The inclusion of any function $F(b)$ should have a correct physics origin. In the above derivation of the $\tilde{W}_{ij}(b,Q,x_A,x_B)$, we added the missing physics (power corrections) to the QCD resummation formalism when $b > b_{max}$. However, we did not include the effect of the partons intrinsic transverse momentum, which should appear as a part of $\tilde{W}_{ij}(b,c/b,x_A,x_B)$ — the boundary condition for evolution equation. When b is small, the factorized formula for the $\tilde{W}_{ij}(b,c/b,x_A,x_B)$ in Eq. (11) should be reliable. But when b is larger than b_{max} or $1/b$ is of the order of the partons intrinsic transverse momentum, the perturbative QCD factorized formula requires a so-called ''Q_T smearing'' to be consistent with experimental data [27]. A Gaussian-like smearing function is often used and does a good job in interpreting the data [27]. In b space, we can include the effect due to the partons nonvanishing intrinsic transverse momentum by choosing

$$F(b) = \exp(-\bar{g}_2 b^2), \tag{35}$$

with a constant $\bar{g}_2$, which should be of order Λ_{QCD}^2. Let $\bar{g}_2 = \Lambda_{\text{QCD}}^2$; we estimate $F(b) \geqslant 0.99$ for $b < b_{max}$, which has literally no effect on the perturbative regime. However, when $b \gg b_{max}$, the $F(b)$ is expected to have a sizable effect on the low energy Drell-Yan data.

To include the corrections due to the partons nonvanishing intrinsic transverse momentum, we modify our extrapolation in Eq. (33) as follows:

$$\tilde{W}^{QZ}(b,Q,x_A,x_B)=\begin{cases}\tilde{W}(b,Q,x_A,x_B), & b\leqslant b_{max},\\ \tilde{W}(b_{max},Q,x_A,x_B)F_{QZ}^{NP}(b,Q,x_A,x_B;b_{max}), & b>b_{max},\end{cases} \tag{36}$$

where the perturbatively calculated $\tilde{W}(b,Q,x_A,x_B)$ is the same as that in Eq. (33). The modified nonperturbative function F_{QZ}^{NP} in Eq. (36) is given by

$$F_{QZ}^{NP}(b,Q,x_A,x_B;b_{max})=\exp\left\{-\ln\left(\frac{Q^2b_{max}^2}{c^2}\right)\{g_1[(b^2)^\alpha-(b_{max}^2)^\alpha]+g_2(b^2-b_{max}^2)\}-\bar{g}_2(b^2-b_{max}^2)\right\}. \tag{37}$$

Although the terms with g_2 and $\bar{g}_2$ have the same b dependence, they have different physics origins. The term with $\bar{g}_2$ represents the effect of the partons nonvanishing intrinsic transverse momentum. The term with g_2 comes from the dynamical power corrections, and has an explicit dependence on Q. In deriving Eq. (36), we neglected the intrinsic transverse momentum corrections $\exp(-\bar{g}_2b^2)$ to $\tilde{W}$ in the perturbative region, which is consistent with keeping only the leading power QCD calculations in this region.

Our extrapolation defined in Eq. (36) clearly separates the calculable perturbative region from the large b nonperturbative region. In addition, all b dependence in Eq. (37) has its their own physics origins. The $(b^2)^\alpha$ dependence mimics the summation of the perturbatively calculable leading power contributions to the kernels K and G to all orders in the running coupling constant $\alpha_s(\mu)$ with the scale μ running into the nonperturbative region [25]. The b^2 dependence is a direct consequence of dynamical power corrections to the renormalization group equations of the kernels K and G. We did not include power corrections to the evolution equation because of our choice of b_{max}. We believe that when Q^2 is much larger than c^2/b_{max}^2, our extrapolation defined in Eq. (36) should give a good description of the b dependence in the region not too much larger than b_{max}, which is most relevant to heavy boson production. Uncertainties for not including higher power corrections can be tested by studying the sensitivities on the parameters g_2 and b_{max} [8].

D. Extrapolation to low Q^2

When we apply our extrapolation defined in Eqs. (36) and (37) to the low Q^2 Drell-Yan data, we might need a few modifications. As discussed in Sec. II, the Fourier transform from b space to Q_T space is sensitive to the large b region when Q^2 and $\sqrt{S}$ are both small. Therefore, the Q_T distributions at low energies are much more sensitive to the parameters g_2 and b_{max} or even higher power corrections.

For deriving our extrapolation, we systematically dropped the power corrections of momentum scale between $1/b_{max}^2$ and Q^2. When Q^2 is small, the leading power perturbative QCD calculations receive relatively larger $1/Q^2$ corrections, in particular, type-2 power corrections. For example, a $1/Q^2$ term in the evolution equation in Eq. (5) results in a type-2 power correction to the perturbatively calculated $\tilde{W}(b,Q,x_A,x_B)$ in Eq. (36). The size of the type-2 power corrections resummed from Λ^2/Q^2 to $\Lambda^2/(1/b_{max}^2)$ is proportional to the numerical value of $b_{max}^2\Lambda^2$, where Λ^2 is the characteristic scale of the power corrections. For a larger b_{max}, the perturbatively calculated $\tilde{W}(b,Q,x_A,x_B)$ receives a larger power correction.

On the other hand, the leading power contributions are resummed from $\ln(1/b_{max}^2)$ to $\ln(Q^2)$, and are proportional to the numerical value of $\ln(Q^2)$. When $Q^2\sim M_Z^2$ at collider energies, the $\ln(Q^2)$ is much larger than the $b_{max}^2\Lambda^2$, and the power corrections to the perturbatively calculated $\tilde{W}(b,Q,x_A,x_B)$ can be neglected. However, at the fixed target energies, both Q^2 and the leading power contributions are much smaller. Therefore, the power corrections to the perturbatively calculated leading power contributions become relatively more important at fixed target energies.

Therefore, in order to reduce the relative size of the power corrections in the perturbative (or small b) region, we need to reduce the numerical value of b_{max}. On the other hand, we prefer to keep the b_{max} as large as possible to have more contributions from the perturbative region in order to have more prediction than parameter fitting. The $b_{max}=0.5\ \mathrm{GeV}^{-1}$ was proposed in Ref. [6]. For our numerical results in Sec. IV, we will test the sensitivities on the choices of b_{max}.

The $\ln(Q^2b_{max}^2/c^2)$ dependence in our F_{QZ}^{NP} is a direct consequence of dropping the type-2 power corrections to the evolution equation in Eq. (5). Therefore, in order to preserve the $\ln(Q^2b_{max}^2/c^2)$ dependence in our extrapolation, we expect to require a smaller b_{max} for a better description of the low energy Drell-Yan data.

IV. NUMERICAL RESULTS AND CONCLUSIONS

In this section, we numerically compare the Q_T distributions derived from the b-space resummation formalism with experimental data from W and Z production at collider energies to the low energy Drell-Yan processes.

A. Numerical accuracy

One of the potential drawbacks of the b-space resummation formalism is the difficulty of matching the resummed and fixed-order predictions to the Q_T distributions at large Q_T [1]. It was generally believed [1] that the b-space resummed Q_T distribution from Eq. (1) becomes unphysical or negative when Q_T is large. For example, a matching between

the resummed and fixed-order calculations has to take place at $Q_T \sim 50$ GeV for W production when these two predictions cross over [14]. On the other hand, as we discussed in Sec. II, we expect the predictions derived from the b-space resummation formalism in Eq. (1) to work better when Q_T is larger because (1) the b integral is dominated by the smaller b region and (2) the perturbatively calculated Y term is larger than the resummed $\tilde{W}$ term. We find that this puzzle was mainly caused by a lack of numerical accuracy of the Bessel function used to perform the Fourier transform in Eq. (17). As we show below, the Q_T distributions derived from the b-space resummation formalism are smoothly consistent with data for all transverse momenta up to Q.

As a result of the oscillatory nature of the Bessel function, a high numerical accuracy of the $J_0(z)$ with $z = Q_T b$ in Eq. (17) is necessary for ensuring an accurate cancellation in the large z region for a reliable b integration. Because z is proportional to Q_T, the number of oscillations of the Bessel function strongly depends on the value of Q_T for the same range of b. For example, when $b \in (0,2)$ GeV^{-1}, $J_0(Q_T b)$ crosses zero 0, 6, and 63 times for $Q_T = 1$, 10, and 100 GeV, respectively. It is clear that numerical accuracy of the Bessel function is extremely important for the large Q_T region. We noticed that most work published in the literature used some kind of asymptotic form to approximate the Bessel function when $z = Q_T b$ is large. We find that the use of an asymptotic form for the Bessel function is a major source of the uncertainties observed for the large Q_T region. Instead of using an asymptotic form, we use the following integral form for the Bessel function:

$$J_0(z) = \frac{1}{\pi}\int_0^{\pi} \cos[z\sin(\theta)]\, d\theta. \tag{38}$$

The great advantage of using an integral form is that we can control the numerical accuracy of the Bessel function by improving the accuracy of the integration in Eq. (38). One can test the numerical accuracy of the Fourier transform in Eq. (17) by using functions whose Fourier transform can be carried out analytically. In view of the nonperturbative b dependence in the large b region, we used two functions $\exp(-\sigma b)$ and $\exp(-b^2/\sigma^2)$ to test the numerical accuracy of the b integration in Eq. (17). The b integration for these two functions can be carried out analytically. Having an analytical solution in Q_T space, we can study the convergence and numerical accuracy of the Fourier transform at different Q_T by varying the parameter σ of these two functions. We find that by using the integral form of the Bessel function, the numerical integration over b defined in Eq. (17) is very accurate for a wide range of σ and Q_T, and the accuracy is only limited by the precision of variables used in a computer programming language.

B. Q_T distributions of W and Z production

In this subsection, we compare the predictions of the b-space resummation formalism with Fermilab data on W and Z production, and quantitatively demonstrate the excellent predictive power of the b-space resummation formalism

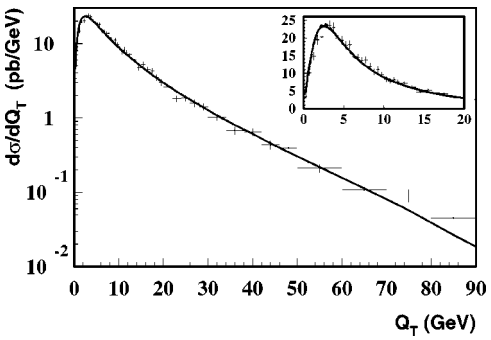

FIG. 7. Comparison between the b-space resummed Q_T distribution and CDF data [29]. The inset shows the $Q_T < 20$ GeV region.

at collider energies [8]. We show that the b-space resummed Q_T distributions are very insensitive to the parameters in the nonperturbative F_{QZ}^{NP}.

Since we are not interested in a detailed fitting to the data in this paper, we did not perform any simulation on final-state cuts to improve the theory curves in the following plots. In all plots, CTEQ4M parton distributions are used, and for the Y term in Eq. (1), we use $\frac{1}{2}\sqrt{Q^2+Q_T^2}$ for the factorization and renormalization scale μ in Eq. (15). For W and Z production, a fixed range of the rapidity was integrated and a narrow width approximation was used for Q^2 integration [28].

We test the sensitivities on the parameters in F_{QZ}^{NP} by first setting $g_2 = 0$ and $\overline{g_2} = 0$ (no ''power'' corrections). We then fix g_1 and α in Eq. (37) by requiring the first and second order derivatives of the $\tilde{W}$ to be continuous at $b = b_{max} = 0.5$ GeV^{-1}, and plot our predictions (solid lines) to the Q_T distributions of Z and W production at Tevatron in Figs. 7 and 8, respectively. In Fig 7, we plot the $d\sigma/dQ_T$ of e^+e^- pairs as a function of Q_T at $\sqrt{S} = 1.8$ TeV. The data are from the CDF Collaboration [29]. Theory curves (Z only) are from Eq. (1) with $\tilde{W}$ given in Eq. (36). The same as in Ref. [29], an overall normalization 1.09 was used. In Fig. 8, we plot $d\sigma/dQ_T$ for W production with the same b_{max} and g_2. The data for W production are from the D0 Collaboration [30]. For the theory curves, we integrate the rapidity of the W particle from -3 to $+3$ and set the overall normalization to be 1. From Figs. 7 and 8, it is clear that the QCD predictions

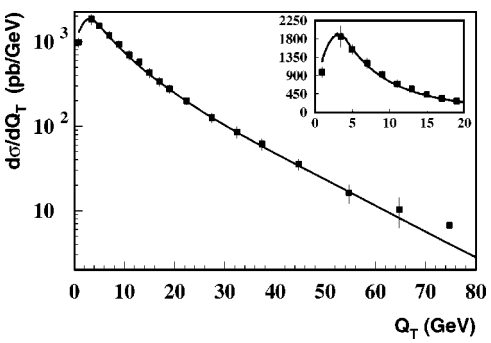

FIG. 8. Comparison between the b-space resummed Q_T distribution and D0 data [30]. The inset shows the $Q_T < 20$ GeV region.

from the b-space resummation formalism are consistent with the data for all $Q_T < Q$.

We notice that the theory curves in Figs. 7 and 8 are slightly below the data at large Q_T. We believe that it is because we have only the leading order contribution to the Y term in Eq. (1). At large Q_T, the Y term dominates. Similar to the fixed-order perturbative calculations, the next-to-leading order contribution will enhance the theoretical predictions [31]. In addition, the inclusion of the virtual photon channel and its interference with the Z channel should shift the peak of the theory curve to a slightly larger Q_T value and make the theory curves closer to the data [12,29].

We now test the theory curves' sensitivities on the parameters of F_{QZ}^{NP}. Since Q is fixed to the mass of the vector boson and the terms with g_2 and $\overline{g_2}$ have the same b dependence, we can simplify the following discussion by rewriting F_{QZ}^{NP} in Eq. (37) for W and Z production as follows [8]:

$$F_{WZ}^{NP}(b,Q,x_A,x_B;b_{max}) = \exp\{-g_1[(b^2)^\alpha-(b_{max}^2)^\alpha]-g_2(b^2-b_{max}^2)\}. \tag{39}$$

We let g_2 in Eq. (39) be a fitting parameter for any given value of b_{max} and fix g_1 and α by the derivatives. Although the fitting prefers $g_2 \sim 0.8$ GeV^2, the Q_T distributions are extremely insensitive to the choices of b_{max} and g_2. The total χ^2 are very stable for $b_{max} \in (0.25,0.8)$ GeV^{-1} and $g_2 \in (0,1.6)$ GeV^2. In Figs. 7 and 8, we also plot the theory curves (dashed lines) with $g_2 = 0.8$ GeV^2 (the best fitting value). Non-vanishing g_2 gives a small improvement to the Q_T distributions at small Q_T. We then vary the value of α in Eq. (39) by requiring only the first order derivative to be continuous at $b = b_{max}$, and find equally good theoretical predictions, except very mild oscillations in the curves at very large Q_T due to the Fourier transform of a less smoother b-space distribution. It is well known that when Q_T is larger, any small kink in the b-space distributions transforms into oscillations in the Q_T distributions due to more rapid oscillations from the Bessel function $J_0(Q_T b)$. The observed insensitivity on b_{max}, g_2, and α is a clear evidence that the b-space resummation formalism is not sensitive to the power corrections at collider energies. That is, at collider energies, a direct extrapolation of the leading power contributions to the large b region [the $(b^2)^\alpha$ term] represents the most relevant b dependence at large b.

To further test the sensitivities on the nonperturbative F^{NP}, we introduce a cutoff b_c to the b-integration in Eq. (17),

$$w(b_c,Q_T) \equiv \frac{1}{2\pi}\int_0^{b_c} dbbJ_0(Q_T b)\tilde{W}^{QZ}(b,Q,x_A,x_B), \tag{40}$$

and define the ratio

$$R(b_c,Q_T) \equiv \frac{w(b_c,Q_T)}{w(b_c=\infty,Q_T)}. \tag{41}$$

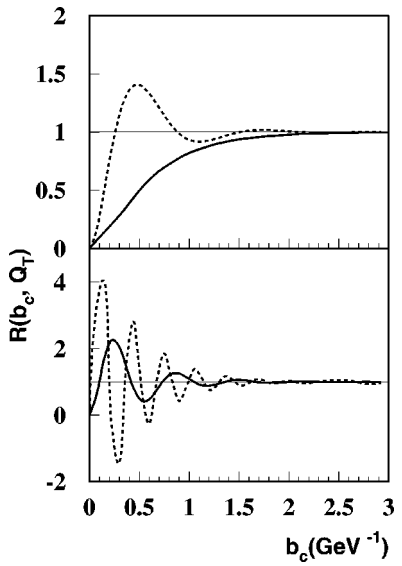

FIG. 9. Ratio $R(b_c,Q_T)$ in Eq. (41) as a function of b_c for Z production at Tevatron energy: $Q_T = 0$ GeV (solid line), $Q_T = 5$ GeV (dashed line) in the top plot; $Q_T = 10$ GeV (solid line), $Q_T = 20$ GeV (dashed line) in the bottom plot.

Because of the oscillatory nature of the Bessel function, we expect the ratio $R(b_c,Q_T)$ to oscillate around 1 and eventually converge to 1 as b_c increases. In Fig. 9, we plot the ratio $R(b_c,Q_T)$ as a function of b_c for Z production at different values of Q_T. In plotting the theory curves in Fig. 9, we set $\sqrt{S} = 1.8$ TeV, $b_{max} = 0.5$ GeV^{-1}, and $g_2 = 0.8$ GeV^2. For $Q_T = 0$, 5, 10, and 20 GeV, as shown in Fig. 9, the $R(b_c,Q_T)$ quickly reaches 1 at $b_c \sim 1/Q_T$ as b_c increases. Even at $Q_T = 0$, $R(b_c,Q_T)$ is close to 1 within a few percent at $b_c \sim 2$ GeV^{-1}. It tells us that the physics of the Q_T distribution is dominated by the perturbative (or small b) region. However, as a result of the oscillatory nature of the Bessel function, the b integral for the Fourier transform in Eq. (1) converges roughly at a common value of $b_c \sim 2$ GeV^{-1}, which is larger than b_{max}. That is, the nonperturbative extrapolation to the large b region is necessary to ensure the correct cancellations in the large b region. The small dependence on the parameters g_2 and b_{max} shows that our extrapolation defined in Eq. (37) catches most of the physics in this region, and higher power corrections are not important.

In addition, we show the quantitative g_2 dependence of the b-space resummed Q_T distributions by introducing the following ratio:

$$R_\sigma(Q_T,g_2) \equiv \frac{d\sigma(g_2)}{dQ^2dydQ_T^2} \Big/ \frac{d\sigma(g_{2_b})}{dQ^2dydQ_T^2}, \tag{42}$$

where $d\sigma/dQ^2dydQ_T^2$ is defined in Eq. (1), and $g_{2_b} = 0.8$ GeV^2 is the best fit value for g_2. In Fig. 10, we plot the ratio $R_\sigma(Q_T,g_2)$ in Eq. (42) as a function of Q_T for Z production at the Tevatron energy. The solid line corresponds to $g_2 = 2g_{2_b}$, while the dashed line has the $g_2 = \frac{1}{2}g_{2_b}$. For almost all $Q_T < Q$, the deviation of the b-space

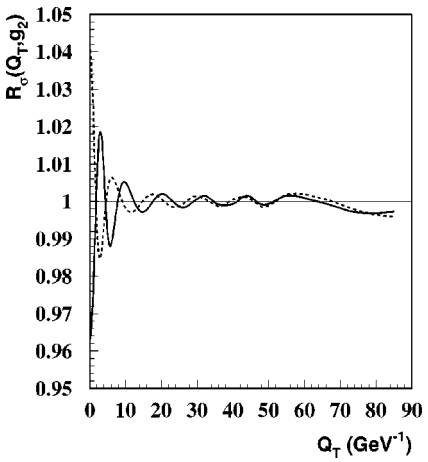

FIG. 10. Ratio $R_\sigma(Q_T,g_2)$ in Eq. (42) at $Q=M_Z$ and $\sqrt{S}=1.8$ TeV as a function of Q_T: $g_2=2g_{2_b}$ (solid line) and $g_2=(1/2)g_{2_b}$ (dashed line).

resummed Q_T distributions at the Tevatron energy is less than 2% when we change g_2 from half to twice the best fit g_2 value. The small irregularity for $Q_T>50$ GeV is due to the fact that the calculated cross section has about half of a percent numerical uncertainty in this region, which is of the same order as the deviation. We find that the deviation at the LHC energy is much less than 1%. That is, the Fourier transform from b space to Q_T space is completely determined by the perturbatively calculated b-space distribution plus our extrapolation, which is totally fixed by the continuity at $b=b_{max}$. Therefore, we conclude that the b-space resummed Q_T distributions for vector boson production at collider energies have excellent predictive power.

C. Drell-Yan Q_T distributions at low energies

As discussed in Sec. II, the Drell-Yan Q_T distributions at fixed target energies are much more sensitive to the nonperturbative input at large b. The predictive power of the b-space resummation formalism may be limited. To explore the predictive power of the b-space resummed Q_T distributions for the low energy Drell-Yan process, we compare the low energy Drell-Yan data with the predictions from the CSS b-space resummation formalism plus the extrapolation defined in Eq. (36). We use a subset of available data to fix the parameters in the nonperturbative F_{QZ}^{NP}, and then, we compare the predictions calculated by using these parameters with the rest of the data.

When $Q_T\leqslant 4$ GeV, the Bessel function does not have any oscillation in the perturbative region ($b<b_{max}$). A less smooth connection of the $\tilde{W}(b,Q,x_A,x_B)$ at $b=b_{max}$ does not produce any apparent oscillation for the Q_T distribution in this region. Therefore, we do not have to require the derivative of $\tilde{W}^{QZ}(b,Q,x_A,x_B)$ in Eq. (36) to be continuous at $b=b_{max}$. In this subsection, we treat g_1, g_2, $\bar{g}_2$, and α in the F_{QZ}^{NP} as fitting parameters. In order to maximize the predictive power of the b-space resummed Q_T distributions, we try to fit the data with the least number of parameters, and then add more parameters to see the improvements. By going through this fitting procedure, we can learn the importance of each parameter and the corresponding physics.

TABLE I. Nonperturbative parameters in the F_{QZ}^{NP} obtained by fitting 28 data points on Drell-Yan Q_T distributions at the fixed target energies.

b_{max} (GeV^{-1})	χ^2	α	g_1 (GeV$^\alpha$)	g (GeV^2)	$N_{\rm E288}$	$N_{\rm E605}$
0.5	78	0.65	0.4	0	0.85	0.9
0.5	32	0.15	1.14	0.19	0.88	0.93
0.4	27	0.15	1.06	0.23	0.93	0.98
0.3	24	0.15	0.92	0.28	0.97	1.00

We choose the following Fermilab data to fit the parameters in the F_{QZ}^{NP}: $Q\in(5,6)$ GeV and $Q\in(7,8)$ GeV from E288 [16], and $Q\in(7,8)$ GeV and $Q\in(10.5,11.5)$ GeV from E605 [32]. We have a cut on the transverse momentum, $Q_T\leqslant 1.4$ GeV, which is the same as that used in Ref. [13]. Since the g_2 dependence is very small at collider energies, we try to fit these Drell-Yan data with two parameters, g_1 and α, plus two overall normalizations for two experiments. Using the F_{QZ}^{NP} in Eq. (37) and $b_{max}=0.5$ GeV^{-1}, we obtain a convergent fit with a total $\chi^2=78$ for 28 data points. The corresponding numerical values of the fitting parameters, g_1, α, and two overall normalization constants for these two experiments are given in Table I. The large χ^2 clearly indicates that power corrections (or terms proportional to b^2 in the F_{QZ}^{NP}) are very important for understanding the low energy data.

We now include the b^2 dependence of the F_{QZ}^{NP} into the fit. In order to use a minimum number of fitting parameters, we first combine both g_2 and $\bar{g}_2$ terms and define

$$g_2\ln\left(\frac{Q^2b_{max}^2}{c^2}\right)+\bar{g}_2\equiv g. \tag{43}$$

We approximate the g as a constant fitting parameter. With three fitting parameters, g_1, α, and g, plus two overall normalizations for two experiments, we fit the same 28 data points for $b_{max}=0.5$ GeV^{-1}. We obtain a much better fit with a total $\chi^2=32$, and the corresponding fitting parameters are given in Table I. Using $b_{max}=0.5$ GeV^{-1} and the numerical values of the fitting parameters in Table I, we find that the b^2 term in F_{QZ}^{NP} is less than the $(b^2)^\alpha$ term for b as large as $b\sim 2.4$ GeV^{-1} (~ 2.0 GeV^{-1} for $b_{max}=0.3$ GeV^{-1}). It indicates that although the power corrections (the b^2 dependence) are important, the extrapolation from the leading power contributions [the $(b^2)^\alpha$ dependence in the F_{QZ}^{NP}] is crucial for understanding the low energy data.

As we discussed in Sec. III D, we can test the size of power corrections to the perturbative region ($b<b_{max}$) by studying the b_{max} dependence. We find that the fitting parameter α is extremely stable when we change the b_{max}, and it prefers a numerical value around $\alpha\sim 0.15$. This can be understood as follows. The parameter α was introduced in Sec. III B to approximate the μ^2 dependence when we ex-

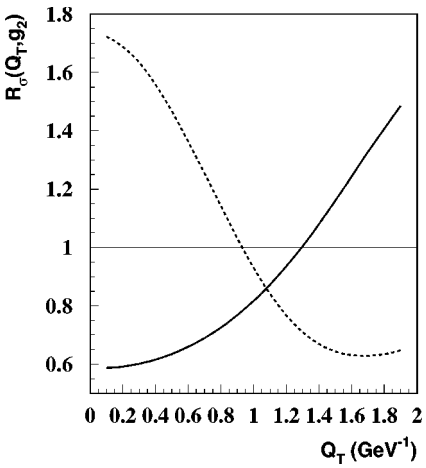

FIG. 11. Same as that in Fig. 10 at $Q=6$ GeV and E288 collision energy.

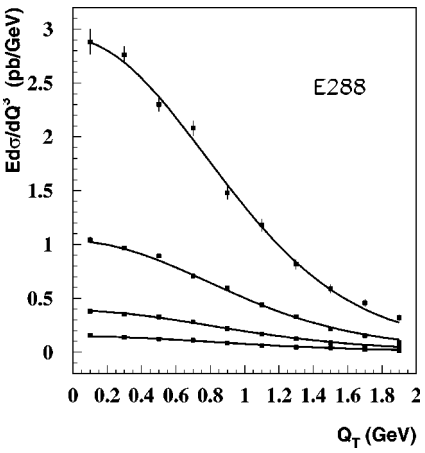

FIG. 12. Comparison between the *b*-space resummed Q_T distribution and Fermilab E288 data [16]. The overall normalization for the theory curves: $N_{\mathrm{E288}}=0.97$.

trapolate the leading power contributions to $S(b,Q)$ into the small μ^2 region [25]. Therefore, the parameter α should only depend on the effective anomalous dimensions [resummed to all orders in the running coupling constant, $\alpha_s(\mu)$], and should not be sensitive to the numerical value of the b_{max}. We then fix $\alpha=0.15$ and re-fit those 28 data points with two parameters, g_1 and g, plus two overall normalization constants.

We find a smooth reduction of the total χ^2 when we decrease the b_{max} to as low as 0.3 GeV^{-1}. For $b_{max}=0.5$, 0.4, and 0.3, we obtain convergent fits with the total $\chi^2=32$, 27, and 24, respectively. The corresponding fitting parameters are listed in Table I. Although the total χ^2 is still very stable when we further reduce b_{max}, we stop at $b_{max}=0.3$ GeV^{-1} because it is difficult to distinguish the perturbative prediction from the parameter fitting when b_{max} is too small. We confirm from the fitting results listed in Table I that the $(b^2)^\alpha$ term in our extrapolation is very important and it dominates the transition region between the perturbative calculation and the nonperturbative extrapolation. We learn that the overall normalizations, which are needed to fit the different experimental data sets, have a strong dependence on the b_{max}. As shown in Table I, the overall normalizations are driven to unity as b_{max} decreases. That is, if we reduce the relative size of the power corrections in the perturbative region ($b<b_{max}$) by a reduction of b_{max}, both data sets used in the fit are in an excellent agreement with each other.

In order to show the quantitative size of the power corrections (the b^2 term in the F_{QZ}^{NP}) at low energy, we replot Fig. 10 at $Q=6$ GeV and $\sqrt{S}=27.4$ GeV in Fig. 11. In plotting Fig. 11, we use the ratio $R_\sigma(Q_T,g_2)$ defined in Eq. (42) with the g_2 dependence replaced by the g dependence defined in Eq. (43). The g_{2_b} in Eq. (42) is replaced by the best fit value g_b. We choose $b_{max}=0.3$ GeV^{-1} and the corresponding fitting parameters: α, g_1, and g given in Table I. The best fit value $g_b=0.28$ GeV^2. In Fig. 11, the solid line corresponds to $g=2g_b$ while the dashed line has $g=\frac{1}{2}g_b$. For Q_T from 0 to 2 GeV, the b^2 dependence can change the *b*-space resummed Q_T distributions by as much as 80% when the parameter g changes from half to twice of the best fit value. In contrast to the 2% deviation at collider energies, as shown in Fig. 10, the large variation shown in Fig. 11 further confirms that the power corrections are very important for describing the Drell-Yan data at the fixed target energies [33].

To explore the predictive power of the *b*-space resummed Q_T distributions at fixed target energies, we compare the resummed Q_T distributions with existing Drell-Yan data in Figs. 12, 13, and 14. All theory curves in these figures are calculated with our extrapolation defined in Eq. (36) and $b_{max}=0.3$ GeV^{-1}. The nonperturbative extrapolation to the large *b* region: F_{QZ}^{NP} is defined in Eq. (37) with the g_2 and $\overline{g_2}$ terms combined as in Eq. (43). We fix the parameter α to be 0.15, and use the fitted values $g_1=0.92$ GeV$^\alpha$ and $g=0.28$ GeV^2 from Table I. Although we only used 28 data points with $Q_T\leqslant 1.4$ GeV in our fits for determining the two parameters, g_1 and g, we plot both theory curves and data for a much enlarged phase space in Figs. 12, 13, and 14. We plot data with Q_T as large as 2 GeV at different values of Q in order to explore the predictive power of the theoretical calculations. In Fig. 12, we compare the theoretical calculations

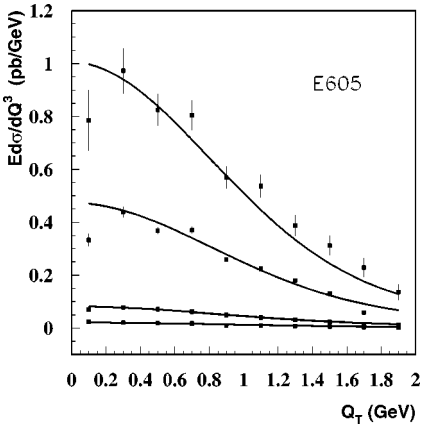

FIG. 13. Comparison between the *b*-space resummed Q_T distribution and Fermilab E605 data [32]. The overall normalization for the theory curves: $N_{\mathrm{E605}}=1.0$.

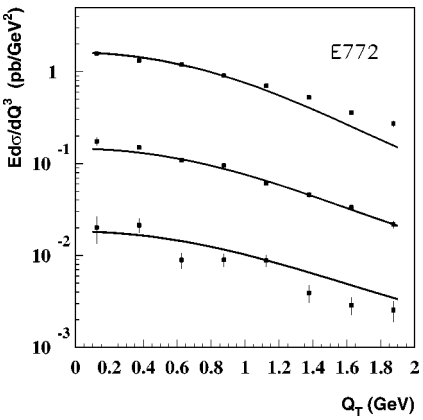

FIG. 14. Comparison between the *b*-space resummed Q_T distribution and Fermilab E772 data [34]. The overall normalization for the theory curves: $N_{\mathrm{E772}}=1.6$.

with Fermilab E288 data at $\sqrt{S}=27.4$ GeV [16]. The theory curves are multiplied by an overall normalization constant $\mathrm{N_{E288}}=0.97$ as listed in Table I, which is different from what was found in Ref. [13]. From top to bottom in Fig. 12, the four curves along with four data sets correspond to $Q \in (5,6)$ GeV, (6,7) GeV, (7,8) GeV, and (8,9) GeV, respectively. Two of the four data sets, $Q \in (5,6)$ GeV and (7,8) GeV with $Q_T<1.4$ GeV, were used in our fitting. That is, only 14 of the 40 data points plotted in Fig. 12 were used in the fitting. Clearly, for all Q_T up to 2 GeV, the *b*-space resummed Q_T distributions are in excellent agreement with the data from E288. In Fig. 13, we plot the resummed Q_T distributions along with Fermilab E605 data [32]. The overall normalization constant for E605 is 1. Exactly the same values of g_1 and g are used for calculating the theory curves in Figs. 12 and 13. In Fig. 13, from top to bottom, the four curves along with four data sets correspond to $Q \in (7,8)$ GeV, (8,9) GeV, (10.5,11.5) GeV, and (13.5,18.0) GeV, respectively. Similar to E288 data, only two of the four data sets, $Q \in (7,8)$ GeV and (10.5,11.5) GeV with $Q_T<1.4$ GeV, were used in our fitting. Although only 14 of the 40 data points in Fig. 13 were used in the fitting, the *b*-space resummed Q_T distributions are in a good agreement with all 40 points, except a few points with $Q \in (7,8)$ GeV. Actually, seven of the ten data points in this set with $Q \in (7,8)$ GeV were used in our fitting. However, because of the relatively large error bars, these data points did not have enough weight in the fitting. Nevertheless, the theory curves calculated with two fitting parameters, g_1 and g, give a very good description of the low energy Drell-Yan data in Figs. 12 and 13. In particular, the overall normalization constants for both experiments are very close to the unity.

As pointed out in Ref. [13], the *b*-space resummed Q_T distributions have to multiply a large overall normalization constant in order to be consistent with the Fermilab E772 data. In Fig. 14, we plot the *b*-space resummed Q_T distributions along with the E772 data [34]. Three data sets from top to bottom correspond to $Q \in (5,6)$ GeV, (8,9) GeV, and (11,12) GeV, respectively. The theory curves are calculated with the same formula and parameters used to calculate the curves in Figs. 12 and 13, except a much larger overall normalization constant $N_{\mathrm{E772}}=1.6$, which is consistent with what was found in Ref. [13]. Although none of these data points in Fig. 14 were used in our fitting, the theory curves describe the data well. Without plotting another figure, we state that the *b*-space resummed Q_T distributions are also consistent with the R209 data [17].

In order to get a feeling on the relative size of the contributions from the partons intrinsic transverse momentum and the dynamical power corrections, we separate the g_2 and $\overline{g_2}$ terms in Eq. (43). With $b_{max}=0.3$ GeV^{-1} and a fixed $\alpha=0.15$, we perform a new fit with three fitting parameters, g_1, g_2, and $\overline{g_2}$. For the same 28 data points, we did not get much improvement in the total χ^2. This result should be expected because (1) we already have an excellent fit with a $\chi^2/N_{\mathrm{DF}}\sim 1$ when g_2 and $\overline{g_2}$ terms is combined, and (2) the range of Q values in our 28 data points are limited. Nevertheless, the fitting result indicates that the g_2 term and the $\overline{g_2}$ term are roughly equal. That is, the effect of the partons intrinsic transverse momentum, which is Q independent, is as important as that of the dynamical power corrections at the fixed target energies.

From all three figures, in Figs. 12, 13, and 14, we conclude that the CSS resummation formalism in combination with our derived extrapolation provides a very good description of the Drell-Yan Q_T distributions at the fixed target energies. Using only 28 data points with $Q_T<1.4$ GeV to fix the parameters, g_1 and g, our numerical results are consistent with over 100 data points from three experiments. In particular, except the E772 data, the overall normalization constants between the theory and the data are extremely close to the unity.

To conclude this subsection, we demonstrate the convergence and stability of the Fourier transform at the fixed target energies by plotting the ratio $R(b_c,Q_T)$ as a function of b_c in Fig. 15. The ratio $R(b_c,Q_T)$, defined in Eq. (41), is evaluated at $Q=6$ GeV and $\sqrt{S}=27.4$ GeV. For calculating the resummed *b*-space distribution $\tilde{W}^{QZ}(b,Q,x_A,x_B)$, we choose $b_{max}=0.3$ GeV^{-1} and the corresponding fitting parameters listed in Table I, which are the same as those used for plotting theory curves in Figs. 12, 13, and 14. In Fig. 15, we plot the ratio $R(b_c,Q_T)$ for four different Q_T values: 0, 0.5, 1.0, and 2.0 GeV. The ratio $R(b_c,Q_T)$ quickly converges to 1 at $b_c\sim 3$ GeV^{-1}. By comparing Fig. 9 and Fig. 15, we conclude that the Fourier transform for the *b*-space resummed Q_T distributions converges at $b_c\sim$ a few GeV^{-1}, and therefore, higher power corrections are not very important. On the other hand, because the Fourier transform converges in the nonperturbative region, a reliable extrapolation from the perturbatively calculated *b*-space distribution at small *b* to the nonperturbative large *b* region is necessary and crucial in order to be consistent with experimental data. From the consistency shown in Figs. 12, 13, and 14, we further conclude that the functional dependence on the impact parameter *b*, introduced in our F^{NP}_{QZ}, catches the correct physics.

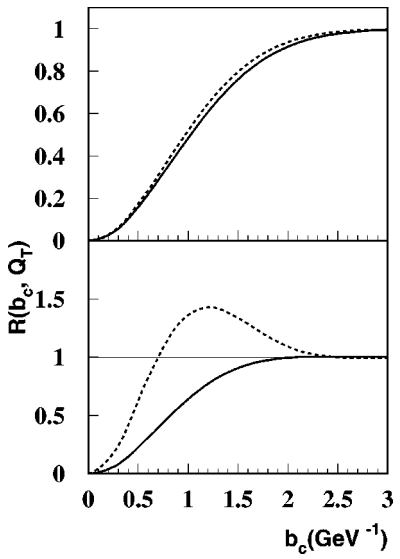

FIG. 15. Ratio $R(b_c,Q_T)$ as a function of b_c for Drell-Yan production at $Q=6$ GeV and $\sqrt{S}=27.4$ GeV: $Q_T=0$ GeV (solid line), $Q_T=0.5$ GeV (dashed line) in the top plot; $Q_T=1$ GeV (solid line) $Q_T=2$ GeV (dashed line) in the bottom plot.

D. Conclusions

In conclusion, we have quantitatively investigated the role of the nonperturbative input in the CSS b-space QCD resummation formalism for the Drell-Yan Q_T distributions at both collider and fixed target energies. We find that the predictive power of the CSS resummation formalism has a strong dependence on the collision energy $\sqrt{S}$. The $\sqrt{S}$ dependence is a consequence of the steep evolution of parton distributions at small x, and it significantly improves the predictive power of the CSS formalism at collider energies, in particular, at the LHC energy. We show that although the resummed Q_T distributions are mostly determined by the perturbatively calculated b-space distributions at small b, a reliable extrapolation to the nonperturbative large b region is necessary to ensure the correct cancellations of the b integration when $b>1/Q_T$. By adding power corrections to the renormalization group equations in the CSS resummation formalism, we derive a new functional form in Eq. (36) to extrapolate the perturbatively resummed b-space distributions to the large b region. We demonstrate that at collider energies, the CSS resummation formalism with our extrapolation has an excellent predictive power for Q_T distributions of W and Z production for Q_T as large as Q. Because of the smooth resummed Q_T distributions, the matching between the resummed and fixed-order calculations at large Q_T is less ambiguous.

In this paper, we have explicitly shown that the power corrections are very important for the resummed Q_T distributions at the fixed target energies. With only two parameters: g_1 and g, obtained by fitting 28 data points, the calculated Q_T distributions using the CSS formalism plus our extrapolation are in a good agreement with all existing data. In our derived extrapolation in Eq. (36), the resummed b-space distributions for $b<b_{max}$ do not include perturbative power corrections, while the nonperturbative extrapolation have both leading power contributions as well as the power corrections. Therefore, by choosing a smaller b_{max}, we effectively move the power corrections to the relatively small b region. We find that by reducing b_{max}, the overall normalization constants for E288 and E605 data sets are driven to the unity. This result not only shows a good consistency between different experiments, but also tells us that the power corrections are very important for describing the low energy Drell-Yan transverse momentum distributions.

Finally, we argue that the CSS b-space resummation formalism should provide a reliable prediction for Higgs boson production at LHC energy. At $\sqrt{S}=14$ TeV, we expect the partonic subprocess, $g+g\rightarrow H+X$, to dominate Higgs boson production when the Higgs boson mass $M_H\sim 115$ GeV. From the fact that $x_A\sim x_B\sim 0.008$ are small and the gluon distribution has a steeper evolution than the quark distribution at small x, we expect the $\sqrt{S}$ dependence of $\tilde{W}(b,Q,x_A,x_B)$ to move the saddle point b_0 to a value much smaller than the $b_{\rm SP}=0.37$ estimated by using Eq. (16), and most likely, even smaller than 0.13 shown in Fig. 3(b) for Z production at LHC energy. Therefore, the b-space QCD resummation formalism should be valid for predicting the Q_T distribution of the hadronic production of Higgs bosons at LHC energy.

ACKNOWLEDGMENTS

We thank P. Nadolsky and C.P. Yuan for help on the LEGACY program package, and thank S. Kuhlmann for help on the experimental data. This work was supported in part by the U.S. Department of Energy under Grant No. DE-FG02-87ER40731.

[1] S. Catani *et al.*, in the Report of the ''1999 CERN Workshop on SM Physics (and more) at the LHC,'' hep-ph/0005025, and references therein.

[2] R. K. Ellis, G. Martinelli, and R. Petronzio, Nucl. Phys. **B211**, 106 (1983); P. Arnold and M. H. Reno, *ibid.* **B319**, 37 (1989); **B330**, 284(E) (1990); P. Arnold, R. K. Ellis, and M. H. Reno, Phys. Rev. D **40**, 912 (1989); R. Gonsalves, J. Pawlowski, and C.-F. Wai, *ibid.* **40**, 2245 (1989).

[3] Y. L. Dokshitzer, D. I. Diakonov, and S. I. Troian, Phys. Rep. **58**, 269 (1980).

[4] G. Parisi and R. Petronzio, Nucl. Phys. **B154**, 427 (1979).

[5] J. C. Collins and D. E. Soper, Nucl. Phys. **B193**, 381 (1981); **B213**, 545(E) (1983); **B197**, 446 (1982).

[6] J. C. Collins, D. E. Soper, and G. Sterman, Nucl. Phys. **B250**, 199 (1985).

[7] S. Catani, E. D'Emilio, and L. Trentadue, Phys. Lett. B **211**, 335 (1988); I. Hinchliffe and S. F. Novaes, Phys. Rev. D **38**, 3475 (1988); R. P. Kauffman, *ibid.* **44**, 1415 (1991); C.-P. Yuan, Phys. Lett. B **283**, 395 (1992).

[8] J.-W. Qiu and X.-F. Zhang, Phys. Rev. Lett. **86**, 2724 (2001);

hep-ph/0012058.
[9] C. T. Davies, B. R. Webber, and W. J. Stirling, Nucl. Phys. **B256**, 413 (1985).
[10] P. B. Arnold and R. P. Kauffman, Nucl. Phys. **B349**, 381 (1991).
[11] G. A. Ladinsky and C. P. Yuan, Phys. Rev. D **50**, 4239 (1994).
[12] R. K. Ellis, D. A. Ross, and S. Veseli, Nucl. Phys. **B503**, 309 (1997).
[13] F. Landry, R. Brock, G. Ladinsky, and C.-P. Yuan, Phys. Rev. D **63**, 013004 (2001).
[14] R. K. Ellis and S. Veseli, Nucl. Phys. **B511**, 649 (1998).
[15] H. L. Lai *et al.*, Phys. Rev. D **55**, 1280 (1997).
[16] E288 Collaboration, A. S. Ito *et al.*, Phys. Rev. D **23**, 604 (1981).
[17] R209 Collaboration, D. Antreasyan *et al.*, Phys. Rev. Lett. **47**, 12 (1981); **48**, 302 (1982).
[18] R. L. Jaffe and M. Soldate, Phys. Lett. **105B**, 467 (1981); Phys. Rev. D **26**, 49 (1982); S. P. Luttrell and S. Wada, Nucl. Phys. **B197**, 290 (1982); R. L. Jaffe, *ibid.* **B229**, 205 (1982).
[19] R. K. Ellis, W. Furmanski, and R. Petronzio, Nucl. Phys. **B207**, 1 (1982); **B212**, 29 (1983); J. Qiu, Phys. Rev. D **42**, 30 (1990).
[20] J.-W. Qiu and G. Sterman, Nucl. Phys. **B353**, 105 (1991); **B353**, 137 (1991).
[21] M. Beneke and V. M. Braun, hep-ph/0010208, and references therein.
[22] O. Nachtmann, Nucl. Phys. **B63**, 237 (1973); H. Georgi and H. D. Politzer, Phys. Rev. D **14**, 1829 (1976).
[23] A. H. Muller and J.-W. Qiu, Nucl. Phys. **B268**, 427 (1986).
[24] J.-W. Qiu, Nucl. Phys. **B291**, 746 (1987).
[25] D. Appell, G. Sterman, and P. Mackenzie, Nucl. Phys. **B309**, 259 (1988).
[26] A. H. Mueller, Nucl. Phys. **B558**, 285 (1999).
[27] J. F. Owens, Rev. Mod. Phys. **59**, 465 (1987).
[28] R. K. Ellis, W. J. Stirling, and B. R. Webber, *QCD and Collider Physics* (Cambridge University Press, Cambridge, England, 1996).
[29] CDF Collaboration, T. Affolder *et al.*, Phys. Rev. Lett. **84**, 845 (2000).
[30] D0 Collaboration, B. Abbott *et al.*, hep-ex/0010026.
[31] P. B. Arnold, R. K. Ellis, and M. H. Reno, Phys. Rev. D **40**, 912 (1989), and references therein.
[32] E605 Collaboration, G. Moreno *et al.*, Phys. Rev. D **43**, 2815 (1991).
[33] X.-F. Guo, J.-W. Qiu, and X.-F. Zhang, Phys. Rev. Lett. **84**, 5049 (2000); Phys. Rev. D **62**, 054008 (2000).
[34] E772 Collaboration, P. L. McGaughey *et al.*, Phys. Rev. D **50**, 3038 (1994).